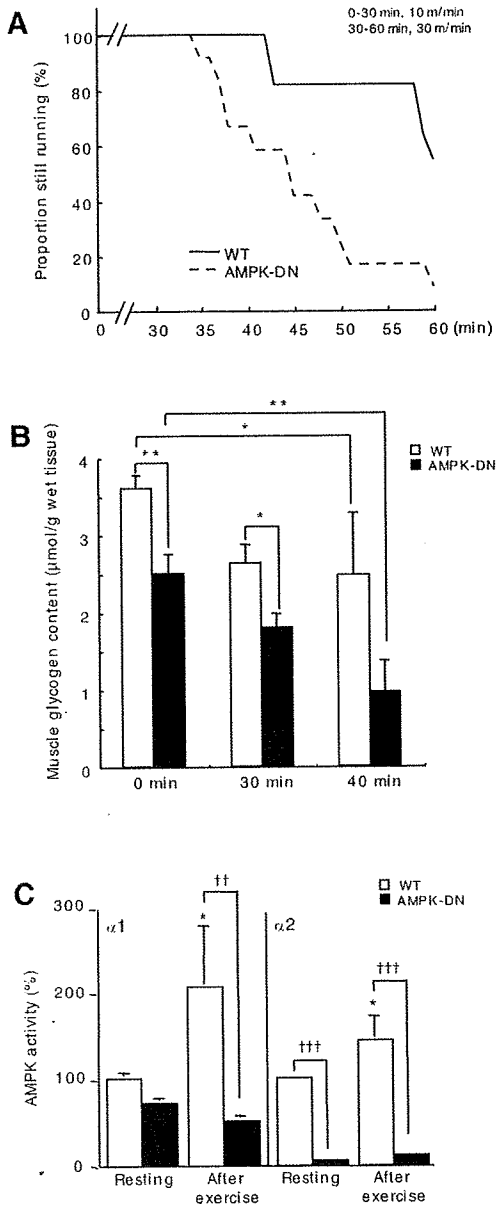

Fig. 3. Exercise tolerance and AMPK activity after low-intensity exercise. *A*: endurance capacity shown as a Kaplan-Meier survival curve. Ten male mice from the α_1-AMPK-DN (line C) and 8 male mice from the WT littermates (each 20 wk old) were exercised by forced running on a treadmill for 30 min at 10 m/min (low-intensity) and then at 30 m/min (high-intensity) for 30 min or until exhaustion. Significant difference ($P = 0.014$, log-rank test) was observed in the endurance capacity of these mice. *B*: glycogen levels in gastrocnemius. Mice were killed at indicated times after initiation of exercise; 40 min indicated 10 min after high-intensity exercise ($n = 3$–7 in each group of mice). $^*P < 0.05$; $^{**}P < 0.01$. *C*: changes in α_1- and α_2-AMPK subunit activities in skeletal muscle (gastrocnemius) from α_1-AMPK-DN (line C) mice and WT littermates after exercise. Skeletal muscles were obtained from α_1-AMPK-DN and WT littermates just after 6 h of low-intensity treadmill exercise (After exercise) or during the resting state (Resting). AMPK activity was measured in immunoprecipitates. Values, expressed as percentage of values in WT littermates, are means ± SE of 5 mice (15 wk old). $^*P < 0.05$ vs. resting mice. $^{\dagger\dagger}P < 0.01$; $^{\dagger\dagger\dagger}P < 0.001$ vs. WT littermates.

their WT littermates (Fig. 3*C*). Compared with the resting state, 6 h of exercise increased α_1-AMPK activity by 2-fold and α_2-AMPK activity by 1.4-fold in WT littermates, whereas the increases in α_1-AMPK and α_2-AMPK activities in response to exercise were not observed in α_1-AMPK-DN mice. Even after a session of exercise, both α_1- and α_2-AMPK activities were still significantly ($P < 0.01$ and $P < 0.001$, respectively) lower in α_1-AMPK-DN (line C) mice when compared with WT mice. Similar results were observed in line E mice (data not shown). In this experiment, α_1-AMPK activity under resting conditions in α_1-AMPK-DN mice tended to be lower but was not significantly different to WT littermates. This might be due to low sample sizes, because the other six independent experiments showed statistically significant reductions in α_1-AMPK activity in α_1-AMPK-DN mice (data not shown). These data indicated that a marked inhibition of α_2-AMPK activities persisted after the session of exercise.

Indirect calorimetry during exercise. To examine which substrate was preferentially utilized during exercise in α_1-AMPK-DN mice, oxygen consumption and carbon dioxide production were monitored during low-intensity exercise and the glucose and lipid oxidation rate were calculated. We examined male and female mice at 2 mo of age (Fig. 4). In a sedentary state, the oxygen consumption and carbon dioxide production did not differ between WT littermates and α_1-AMPK-DN mice in either male or female specimens. Although data obtained at the beginning of exercise were affected by rapid gas exchange in the lung, the low-intensity exercise increased both the oxygen consumption and carbon dioxide production by 1.2- to 1.4-fold in both WT and α_1-AMPK-DN mice, irrespective of sex. Calculated RQ ratio, glucose oxidation rate, lipid oxidation rate, and energy production rate while the mice were sedentary and during exercise did not differ between the WT and α_1-AMPK-DN mice in either male or female specimens. We repeated the same experiments on mice at 6 mo of age and found that both groups of mice could increase lipid oxidation in response to low-intensity exercise (data not shown). There were no significant differences in exercise effects on plasma free fatty acids (FFA) concentrations between WT littermates and α_1-AMPK-DN mice. After 1 h of low-intensity exercise, FFA concentrations were increased from 0.37 ± 0.06 to 0.53 ± 0.04 meq/l ($n = 7$) in WT littermates and from 0.28 ± 0.04 to 0.48 ± 0.08 ($n = 6$) in α_1-AMPK-DN mice, respectively. These data suggest that while sedentary and during low-intensity exercise, glucose and lipid oxidation did not differ in between WT littermates and α_1-AMPK-DN mice.

Palmitate oxidation in isolated skeletal muscles. To measure the rate of fatty acid oxidation in skeletal muscle during exercise directly, production of $^{14}CO_2$ from [^{14}C]palmitate was measured ex vivo using isolated muscle obtained immediately after low-intensity exercise (10 m/min) for 30 min (Fig. 5). In soleus muscle (type I, slow-twitch muscle), the basal rate of palmitate oxidation was not impaired in α_1-AMPK-DN mice. Low-intensity exercise increased the rate of palmitate oxidation by 1.3-fold both in WT littermates and α_1-AMPK-DN mice. The increase in fatty acid oxidation was observed in another type of skeletal muscle, EDL, known as a type II rich fiber muscle. In EDL muscle, the increase in palmitate oxidation in response to low-intensity exercise was 1.4-fold. There was no discernable difference between WT littermates and

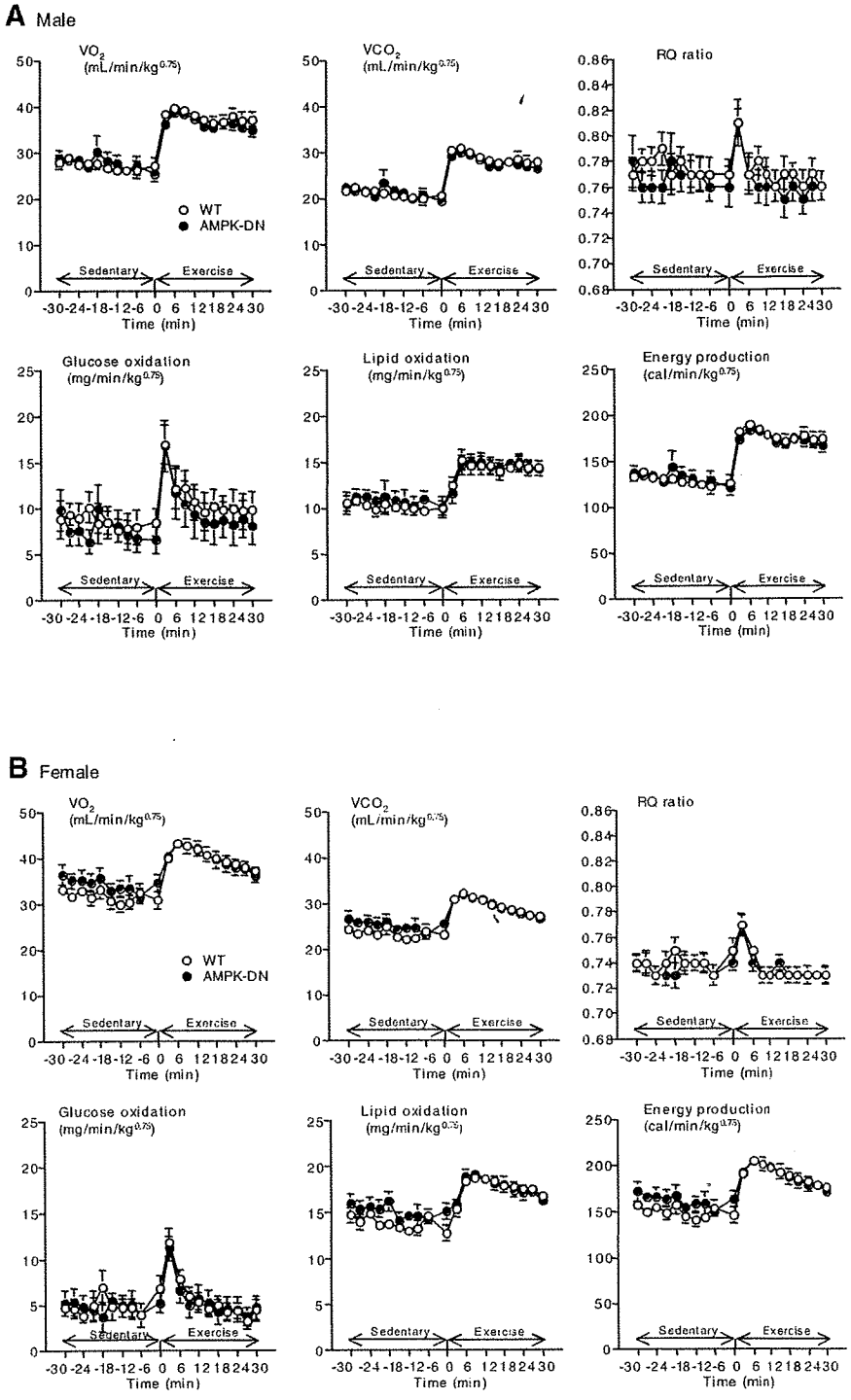

Fig. 4. Calculated glucose and lipid oxidation rate and energy production rate during low-intensity exercise in WT littermates and α_1-AMPK-DN mice. Male (*A*) and female (*B*) α_1-AMPK-DN (C line) and WT (2 mo old) mice started on the treadmill at a speed of 10 m/min (low-intensity exercise) at *time 0*. Oxygen consumption and carbon dioxide production were monitored using an O_2/CO_2 metabolism measuring system for small animals equipped with air-tight treadmill chamber. Data of oxygen consumption and carbon dioxide production were collected for a total of 60 min, while mice were sedentary and during exercise each for 30-min interval. Calculated RQ ratio, glucose and lipid oxidation rate, and energy production rate are also shown. Values are means ± SE of 7–10 mice. Similar results were obtained in α_1-AMPK-DN (line E) mice (data not shown). No significant difference was observed between α_1-AMPK-DN vs. WT littermates.

α_1-AMPK-DN mice for palmitate oxidation in response to low-intensity exercise. These data suggest that the deficiency of α_2-AMPK activity in skeletal muscle did not affect the rate of fatty acid oxidation in response to low-intensity exercise.

DISCUSSION

A low-intensity exercise session increased fatty acid oxidation in α_2-AMPK-deficient α_1-AMPK-DN transgenic mice in vivo and ex vivo, suggesting that activation of α_2-AMPK is not necessary for increased fatty acid oxidation in response to low-intensity exercise. Since changes in RQ ratio and oxygen utilization in the fasting state were not altered between α_1-AMPK-DN transgenic mice and WT littermates, α_2-AMPK in skeletal muscle might not play a major role in the shift to fatty acid oxidation from glucose oxidation under fasting conditions. A similar decrease in body weight in response to fasting (no

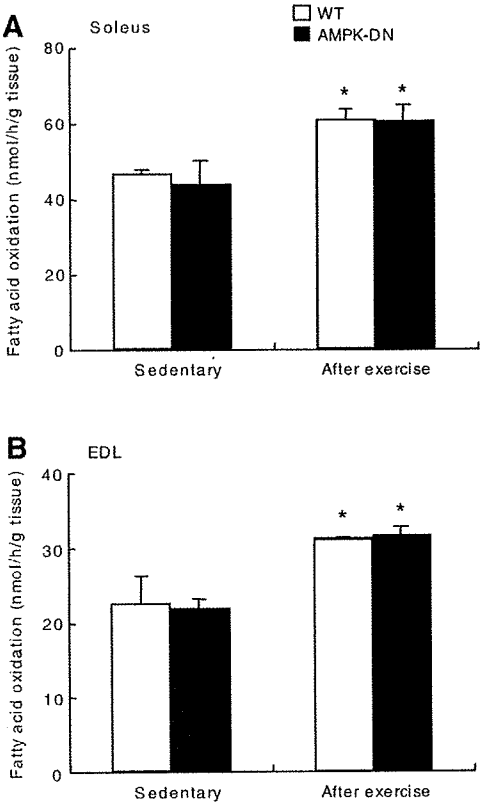

Fig. 5. Palmitate oxidation in isolated soleus (*A*) and EDL (*B*) muscle strips before and after exercise. Male α_1-AMPK-DN (line C) mice and WT littermates (2 mo old) were assigned to the two groups. One group was kept sedentary, while the other group was subjected to the treadmill at a speed of 10 m/min for 30 min. Dissected muscles were immediately used for the measurement of palmitate oxidation. Values are means ± SE of 3 mice. $^*P < 0.05$ vs. sedentary. No significant difference is observed between α_1-AMPK-DN vs. WT littermates.

energy intake) also suggested that energy expenditure was not altered in α_1-AMPK-DN transgenic mice.

Our data are in good agreement with an observation that swimming increased oleate oxidation in EDL from AMPK mutant-overexpression *Tg-Prkag3*^{225Q} mice and AMPK γ_3-knockout mice, similarly to that observed from WT mice (3). EDL is glycolytic (white, fast-twitch type II) muscles. Normal fatty acid oxidation in soleus (red, slow-twitch-type I) muscles in response to low-intensity exercise was also observed in α_1-AMPK-DN mice (Fig. 5*B*), suggesting that α_2-AMPK activity is not essential for an increase in fatty acid oxidation during low-intensity exercise, irrespective of fiber type. In humans, there was a discrepancy between ACC phosphorylation (a marker of AMPK activation) and fatty acid oxidation. A high-intensity exercise session increased ACC phosphorylation in the vastus lateralis muscle; however, fatty acid oxidation was not increased with increasing exercise intensity (9). In prolonged low-intensity exercise (45% of maximum oxygen consumption), ACC phosphorylation in the vastus lateralis muscle was reduced, whereas fatty acid oxidation increased (43). In perfused rat hindquarters, low-intensity muscle contraction by electrical stimulation of sciatic nerve induced an increase in fatty acid oxidation and a reduction in malonyl CoA muscle content without changes in AMPK activation and ACC activities, also suggesting that AMPK activation is not critical in the regulation of fatty acid oxidation during low-intensity muscle contraction (32). AICAR may increase fatty acid oxidation via AMPK activation (26), but low-intensity exercise increases fatty acid oxidation via AMPK-independent mechanism.

Malonyl-CoA is a potent inhibitor of CPT1 (25). AMPK may enhance fatty acid oxidation in skeletal muscles, as in the liver, by inactivation of ACC via phosphorylation, thereby reducing the synthesis of malonyl-CoA (42), and by activation of malonyl-CoA decarboxylase, the enzyme converting malonyl-CoA to acetyl-CoA (29). The importance of ACC2 was supported from the finding that ACC2-knockout mice exhibited increased fat oxidation and reduced fat storage (1). However, malonyl-CoA does not exclusively account for the reduction of all fat oxidation. CPT1 activity was also modified by cytosolic acetyl CoA, carnitine, and pH (21). Other factors that may affect fatty acid oxidation include the fatty acid concentration, proteins that regulate fatty acid transport, and blood flow (21). It is possible that these factors may contribute to an increase in fatty acid oxidation during low-intensity exercise.

Activation of α_2-AMPK was not essential for increased fatty acid oxidation in response to low-intensity exercise, raising the possibility that α_1-AMPK may play a regulatory role. A substantial amount of α_1-AMPK remained in α_1-AMPK DN mice both in a sedentary state and after low-intensity exercise (Figs. 1*B* and 3*C*). It was proposed that residual α_1-AMPK activity in the α_2-AMPK-DN mice may largely stem from nonmuscle α_1-AMPK activity and that the partial reduction in α_1-AMPK activity in α_2-AMPK DN mice could reflect a marked reduction of α_1-AMPK activity in muscle cells (13, 28). If this is the case, α_1-AMPK is not essential for increased fatty acid oxidation in response to low-intensity exercise, either. However, using α_1-AMPK knockout mice, it was recently reported (17) that the increase in α_1-AMPK activity in soleus muscle was required for increased glucose uptake in response to ex vivo twitch contraction. Although it is unknown whether low-intensity twitch contraction ex vivo is relevant to low-intensity exercise in vivo, it is also conceivable that α_1-AMPK might be involved in an increased fatty acid oxidation in response to low-intensity exercise.

Intolerance of exercise is observed in various metabolic conditions. In humans, depletion of muscle glycogen results in fatigue and impaired muscle performance and is a major determinant of endurance (16). However, in mice, it is shown that muscle glycogen is not essential for exercise, since glycogen null mice (the MGSKO mouse that disrupted the muscle isoform of glycogen synthase) do not exhibit impaired exercise tolerance compared with their WT littermates (31). In addition, a genetically modified mouse model (GSL30), which overaccumulates glycogen due to overexpression of a hyperactive form of glycogen synthase, does not possess improved exercise performance (30). Therefore, although we observed a reduction in glycogen content before and after exercise in α_1-AMPK-DN relative to WT littermates, it is not clear that compromised carbohydrate availability in α_1-AMPK-DN mice was a mechanism by which these animals lack high-intensity exercise tolerance. Mice with muscle-specific disruption of the gene encoding the GLUT4 have normal muscle glycogen levels but are impaired in their ability to exercise (38). Expression of

GLUT4 measured by Northern blots in gastrocnemius did not differ between α_1-AMPK-DN mice (99 ± 5%, n = 7) and WT littermates (100 ± 4%, n = 7). Switching to more oxidative muscle fibers may lead to an increase in exercise endurance (39). Expressions of COX2 and COX4 mRNA (mitochondrial enzymes rich in oxidative muscle fibers) in gastrocnemius did not differ between α_1-AMPK-DN mice and WT littermates in this study [COX2: 100 ± 2% (n = 7) in WT littermates and 113 ± 2% (n = 7) in α_1-AMPK-DN mice; COX4: 100 ± 4% (n = 7) in WT littermates and 110 ± 1% (n = 7) in α_1-AMPK-DN mice]. The reason for intolerance in high-intensity exercise observed in α_1-AMPK-DN mice is unclear at present.

In humans, peripheral lipolysis was stimulated maximally at the lowest exercise intensity (25% of maximal oxygen consumption), whereas plasma glucose tissue uptake and muscle glycogen oxidation increased in relation to exercise intensity (34). However, prolonged low-intensity exercise (30% of maximal oxygen consumption) increased FFA oxidation progressively, while glucose oxidation was reduced (2). Therefore, fatty acid oxidation in low-intensity exercise is physiologically important for reduction of fat mass and its mechanism should be clarified. In summary, we suggest that an increased α_2-AMPK activity is not essential for increased skeletal muscle fatty acid oxidation during endurance exercise.

GRANTS

This work was supported in part by Grants-in-Aid for Scientific Research (KAKENHI) from the Japanese Ministry of Education, Culture, Sports, Science and Technology (MEXT, Tokyo); by research grants from the Japanese Ministry of Health, Labor and Welfare (Tokyo); and by a grant from the Promotion of Fundamental Studies in Health Sciences of the National Institute of Biomedical Innovation, Japan. C. R. Bruce is supported by a Peter Doherty postdoctoral fellowship and M. A. Febbraio a Principal Research Fellowship from the National Health and Medical Research Council of Australia.

REFERENCES

1. **Abu-Elheiga L, Matzuk MM, Abo-Hashema KA, Wakil SJ.** Continuous fatty acid oxidation and reduced fat storage in mice lacking acetyl-CoA carboxylase 2. *Science* 291: 2613–2616, 2001.
2. **Ahlborg G, Felig P, Hagenfeldt L, Hendler R, Wahren J.** Substrate turnover during prolonged exercise in man. Splanchnic and leg metabolism of glucose, free fatty acids, and amino acids. *J Clin Invest* 53: 1080–1090, 1974.
3. **Barnes BR, Long YC, Steiler TL, Leng Y, Galuska D, Wojtaszewski JF, Andersson L, Zierath JR.** Changes in exercise-induced gene expression in 5′-AMP-activated protein kinase gamma3-null and gamma3 R225Q transgenic mice. *Diabetes* 54: 3484–3489, 2005.
4. **Birk JB, Wojtaszewski JF.** Predominant alpha2/beta2/gamma3 AMPK activation during exercise in human skeletal muscle. *J Physiol* 577: 1021–1032, 2006.
5. **Bolster DR, Crozier SJ, Kimball SR, Jefferson LS.** AMP-activated protein kinase suppresses protein synthesis in rat skeletal muscle through down-regulated mammalian target of rapamycin (mTOR) signaling. *J Biol Chem* 277: 23977–23980, 2002.
6. **Brennan KJ, Hardeman EC.** Quantitative analysis of the human alpha-skeletal actin gene in transgenic mice. *J Biol Chem* 268: 719–725, 1993.
7. **Bruce CR, Brolin C, Turner N, Cleasby ME, van der Leij FR, Cooney GJ, Kraegen EW.** Overexpression of carnitine palmitoyltransferase I in skeletal muscle in vivo increases fatty acid oxidation and reduces triacylglycerol esterification. *Am J Physiol Endocrinol Metab* 292: E1231–E1237, 2007.
8. **Cahill GF Jr.** Starvation in man. *N Engl J Med* 282: 668–675, 1970.
9. **Chen ZP, Stephens TJ, Murthy S, Canny BJ, Hargreaves M, Witters LA, Kemp BE, McConell GK.** Effect of exercise intensity on skeletal muscle AMPK signaling in humans. *Diabetes* 52: 2205–2212, 2003.
10. **Douen AG, Ramlal T, Rastogi S, Bilan PJ, Cartee GD, Vranic M, Holloszy JO, Klip A.** Exercise induces recruitment of the "insulin-responsive glucose transporter." Evidence for distinct intracellular insulin- and exercise-recruitable transporter pools in skeletal muscle. *J Biol Chem* 265: 13427–13430, 1990.
11. **Dyck JR, Gao G, Widmer J, Stapleton D, Fernandez CS, Kemp BE, Witters LA.** Regulation of 5′-AMP-activated protein kinase activity by the noncatalytic beta and gamma subunits. *J Biol Chem* 271: 17798–17803, 1996.
12. **Ferrannini E.** The theoretical bases of indirect calorimetry: a review. *Metabolism* 37: 287–301, 1988.
13. **Fujii N, Hirshman MF, Kane EM, Ho RC, Peter LE, Seifert MM, Goodyear LJ.** AMP-activated protein kinase α2 activity is not essential for contraction- and hyperosmolarity-induced glucose transport in skeletal muscle. *J Biol Chem* 280: 39033–39041, 2005.
14. **Goodyear LJ, Hirshman MF, Horton ES.** Exercise-induced translocation of skeletal muscle glucose transporters. *Am J Physiol Endocrinol Metab* 261: E795–E799, 1991.
15. **Hardie DG, CarlingD, Carlson M.** The AMP-activated/SNF1 protein kinase subfamily: metabolic sensors of the eukaryotic cell? *Annu Rev Biochem* 67: 821–855, 1998.
16. **Holloszy JO, Kohrt WM, Hansen PA.** The regulation of carbohydrate and fat metabolism during and after exercise. *Front Biosci* 3: D1011–D1027, 1998.
17. **Jensen TE, Schjerling P, Viollet B, Wojtaszewski JF, Richter EA.** AMPK alpha1 activation is required for stimulation of glucose uptake by twitch contraction, but not by H2O2, in mouse skeletal muscle. *PLoS ONE* 3: e2102, 2008.
18. **Johnson LN, Noble ME, Owen DJ.** Active and inactive protein kinases: structural basis for regulation. *Cell* 85: 149–158, 1996.
19. **Jorgensen SB, Viollet B, Andreelli F, Frosig C, Birk JB, Schjerling P, Vaulont S, Richter EA, Wojtaszewski JF.** Knockout of the alpha2 but not alpha1 5′-AMP-activated protein kinase isoform abolishes 5-amino-imidazole-4-carboxamide-4-carboxamide-1-beta-4-ribofuranoside but not contraction-induced glucose uptake in skeletal muscle. *J Biol Chem* 279: 1070–1079, 2004.
20. **Jorgensen SB, Wojtaszewski JF, Viollet B, Andreelli F, Birk JB, Hellsten Y, Schjerling P, Vaulont S, Neufer PD, Richter EA, Pilegaard H.** Effects of alpha-AMPK knockout on exercise-induced gene activation in mouse skeletal muscle. *FASEB J* 19: 1146–1148, 2005.
21. **Kiens B.** Skeletal muscle lipid metabolism in exercise and insulin resistance. *Physiol Rev* 86: 205–243, 2006.
22. **Lowry OH, Passonneau JV.** *A Flexible System of Enzymatic Analysis.* London: Academic, 1972, p. 1–291.
23. **Luiken JJ, Coort SL, Willems J, Coumans WA, Bonen A, van der Vusse GJ, Glatz JF.** Contraction-induced fatty acid translocase/CD36 translocation in rat cardiac myocytes is mediated through AMP-activated protein kinase signaling. *Diabetes* 52: 1627–1634, 2003.
24. **Mahlapuu M, Johansson C, Lindgren K, Hjälm G, Barnes BR, Krook A, Zierath JR, Andersson L, Marklund S.** Expression profiling of the γ-subunit isoforms of AMP-activated protein kinase suggests a major role for γ3 in white skeletal muscle. *Am J Physiol Endocrinol Metab* 286: E194–E200, 2004.
25. **McGarry JD, Mills SE, Long CS, Foster DW.** Observations on the affinity for carnitine, and malonyl-CoA sensitivity, of carnitine palmitoyltransferase I in animal and human tissues. Demonstration of the presence of malonyl-CoA in non-hepatic tissues of the rat. *Biochem J* 214: 21–28, 1983.
26. **Merrill GF, Kurth EJ, Hardie DG, Winder WW.** AICA riboside increases AMP-activated protein kinase, fatty acid oxidation, and glucose uptake in rat muscle. *Am J Physiol Endocrinol Metab* 273: E1107–E1112, 1997.
27. **Miura S, Kai Y, Ono M, Ezaki O.** Overexpression of peroxisome proliferator-activated receptor gamma coactivator-1alpha down-regulates GLUT4 mRNA in skeletal muscles. *J Biol Chem* 278: 31385–31390, 2003.
28. **Mu J, Brozinick JT Jr, Valladares O, Bucan M, Birnbaum MJ.** A role for AMP-activated protein kinase in contraction- and hypoxia-regulated glucose transport in skeletal muscle. *Mol Cell* 7: 1085–1094, 2001.
29. **Park H, Kaushik VK, Constant S, Prentki M, Przybytkowski E, Ruderman NB, Saha AK.** Coordinate regulation of malonyl-CoA decarboxylase, sn-glycerol-3-phosphate acyltransferase, and acetyl-CoA carboxylase by AMP-activated protein kinase in rat tissues in response to exercise. *J Biol Chem* 277: 32571–32577, 2002.
30. **Pederson BA, Cope CR, Irimia JM, Schroeder JM, Thurberg BL, Depaoli-Roach AA, Roach PJ.** Mice with elevated muscle glycogen

stores do not have improved exercise performance. *Biochem Biophys Res Commun* 331: 491–496, 2005.

31. **Pederson BA, Cope CR, Schroeder JM, Smith MW, Irimia JM, Thurberg BL, DePaoli-Roach AA, Roach PJ.** Exercise capacity of mice genetically lacking muscle glycogen synthase: in mice, muscle glycogen is not essential for exercise. *J Biol Chem* 280: 17260–17265, 2005.
32. **Raney MA, Yee AJ, Todd MK, Turcotte LP.** AMPK activation is not critical in the regulation of muscle FA uptake and oxidation during low-intensity muscle contraction. *Am J Physiol Endocrinol Metab* 288: E592–E598, 2005.
33. **Rasmussen BB, Wolfe RR.** Regulation of fatty acid oxidation in skeletal muscle. *Annu Rev Nutr* 19: 463–484, 1999.
34. **Romijn JA, Coyle EF, Sidossis LS, Gastaldelli A, Horowitz JF, Endert E, Wolfe RR.** Regulation of endogenous fat and carbohydrate metabolism in relation to exercise intensity and duration. *Am J Physiol Endocrinol Metab* 265: E380–E391, 1993.
35. **Stein SC, Woods A, Jones NA, Davison MD, Carling D.** The regulation of AMP-activated protein kinase by phosphorylation. *Biochem J* 345: 437–443, 2000.
36. **Toyoda T, Tanaka S, Ebihara K, Masuzaki H, Hosoda K, Sato K, Fushiki T, Nakao K, Hayashi T.** Low-intensity contraction activates the alpha1-isoform of 5′-AMP-activated protein kinase in rat skeletal muscle. *Am J Physiol Endocrinol Metab* 290: E583–E590, 2006.
37. **Viollet B, Andreelli F, Jorgensen SB, Perrin C, Geloen A, Flamez D, Mu J, Lenzner C, Baud O, Bennoun M, Gomas E, Nicolas G, Wojtaszewski JF, Kahn A, Carling D, Schuit FC, Birnbaum MJ, Richter EA, Burcelin R, Vaulont S.** The AMP-activated protein kinase alpha2 catalytic subunit controls whole-body insulin sensitivity. *J Clin Invest* 111: 91–98, 2003.
38. **Wallberg-Henriksson H, Zierath JR.** GLUT4: A key player regulating glucose homeostasis? Insights from transgenic and knockout mice (review). *Mol Membr Biol* 18: 205–211, 2001.
39. **Wang YX, Zhang CL, Yu RT, Cho HK, Nelson MC, Bayuga-Ocampo CR, Ham J, Kang H, Evans RM.** Regulation of muscle fiber type and running endurance by PPARdelta. *PLoS Biol* 2: e294, 2004.
40. **Weir JB.** New methods for calculating metabolic rate with special reference to protein metabolism. *J Physiol* 109: 1–9, 1949.
41. **Winder WW.** Intramuscular mechanisms regulating fatty acid oxidation during exercise. *Adv Exp Med Biol* 441: 239–248, 1998.
42. **Winder WW, Wilson HA, Hardie DG, Rasmussen BB, Hutber CA, Call GB, Clayton RD, Conley LM, Yoon S, Zhou B.** Phosphorylation of rat muscle acetyl-CoA carboxylase by AMP-activated protein kinase and protein kinase A. *J Appl Physiol* 82: 219–225, 1997.
43. **Wojtaszewski JF, Mourtzakis M, Hillig T, Saltin B, Pilegaard H.** Dissociation of AMPK activity and ACCbeta phosphorylation in human muscle during prolonged exercise. *Biochem Biophys Res Commun* 298: 309–316, 2002.
44. **Woods A, Azzout-Marniche D, Foretz M, Stein SC, Lemarchand P, Ferre P, Foufelle F, Carling D.** Characterization of the role of AMP-activated protein kinase in the regulation of glucose-activated gene expression using constitutively active and dominant negative forms of the kinase. *Mol Cell Biol* 20: 6704–6711, 2000.

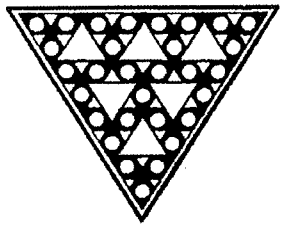

THE JOURNAL OF BIOLOGICAL CHEMISTRY VOL. 284, NO. 3, pp. 1803–1812, January 16, 2009

Rimonabant Ameliorates Insulin Resistance via both Adiponectin-dependent and Adiponectin-independent Pathways*

Received for publication, September 15, 2008, and in revised form, October 23, 2008 Published, JBC Papers in Press, November 13, 2008, DOI 10.1074/jbc.M807120200

Taku Watanabe,[a,b] Naoto Kubota,[a,c,d] Mitsuru Ohsugi,[a] Tetsuya Kubota,[a,c,e] Iseki Takamoto,[a,c] Masato Iwabu,[a] Motoharu Awazawa,[a,d] Hisayuki Katsuyama,[a,d] Chiaki Hasegawa,[f] Kumpei Tokuyama,[f] Masao Moroi,[e] Kaoru Sugi,[e] Toshimasa Yamauchi,[a,c] Tetsuo Noda,[g] Ryozo Nagai,[c,h] Yasuo Terauchi,[i] Kazuyuki Tobe,[j] Kohjiro Ueki,[a,c] and Takashi Kadowaki[a,c,d,1]

From the [a]Department of Diabetes and Metabolic Diseases and [h]Department of Cardiovascular Diseases, Graduate School of Medicine, and the [c]Translational Systems Biology and Medicine Initiative, University of Tokyo, Tokyo 113-8655, Japan, [b]First Department of Medicine, Hokkaido University School of Medicine, Sapporo, Hokkaido 060-8648, Japan, [d]Division of Applied Nutrition, National Institute of Health and Nutrition, Tokyo 162-8636, Japan, [e]Division of Cardiovascular Medicine, Toho University, Ohashi Hospital, Tokyo 153-8515, Japan, [f]Graduate School of Comprehensive Human Sciences, University of Tsukuba, Tsukuba 305-0006, Japan, [g]Department of Cell Biology, Japanese Foundation for Cancer Research, Cancer Institute, Tokyo 135-8550, Japan, the [i]Department of Diabetes and Endocrinology, Yokohama City University School of Medicine, Kanagawa 236-0004, Japan, and the [j]First Department of Internal Medicine, Faculty of Medicine, University of Toyama, Toyama 930-0194, Japan

Rimonabant has been shown to not only decrease the food intake and body weight but also to increase serum adiponectin levels. This increase of the serum adiponectin levels has been hypothesized to be related to the rimonabant-induced amelioration of insulin resistance linked to obesity, although experimental evidence to support this hypothesis is lacking. To test this hypothesis experimentally, we generated adiponectin knock-out (*adipo*(−/−))ob/ob mice. After 21 days of 30 mg/kg rimonabant, the body weight and food intake decreased to similar degrees in the ob/ob and *adipo*(−/−)-ob/ob mice. Significant improvement of insulin resistance was observed in the ob/ob mice following rimonabant treatment, associated with significant up-regulation of the plasma adiponectin levels, in particular, of high molecular weight adiponectin. Amelioration of insulin resistance in the ob/ob mice was attributed to the decrease of glucose production and activation of AMP-activated protein kinase (AMPK) in the liver induced by rimonabant but not to increased glucose uptake by the skeletal muscle. Interestingly, the rimonabant-treated *adipo*(−/−)ob/ob mice also exhibited significant amelioration of insulin resistance, although the degree of improvement was significantly lower as compared with that in the ob/ob mice. The effects of rimonabant on the liver metabolism, namely decrease of glucose production and activation of AMPK, were also less pronounced in the *adipo*(−/−)-ob/ob mice. Thus, it was concluded that rimonabant ameliorates insulin resistance via both adiponectin-dependent and adiponectin-independent pathways.

The prevalence of obesity has increased dramatically in recent years (1, 2). It is commonly associated with type 2 diabetes, coronary artery disease, and hypertension, and the coexistence of these diseases in subjects has been termed the metabolic syndrome (3). There is a demand for effective and safe anti-obesity agents that can produce and maintain weight loss and improve the metabolic syndrome.

The newly discovered endocannabinoid system, consisting of the CB-1 (cannabinoid type-1) receptor and endogenous lipid-derived ligands, contributes to the physiological regulation of energy balance, food intake, and lipid and glucose metabolism, through both central orexigenic effects and peripheral metabolic effects (4–11). The endocannabinoid system is overactivated in genetic animal models of obesity (4, 6), and the selective CB-1 blocker, rimonabant, produces weight loss and ameliorates metabolic abnormalities in obese animals (12, 13). Patients with obesity and hyperglycemia associated with type 2 diabetes exhibit higher concentrations of endocannabinoids in the visceral fat and serum, respectively, than the corresponding controls (14). Rimonabant has been shown to produce substantial weight loss and reduction of waist circumference and also improve insulin resistance and the profile of several metabolic and cardiovascular risk factors in diabetic as well as nondiabetic obese patients (15–18).

Adiponectin is an adipokine that is specifically and abundantly expressed in the adipose tissue and released into the circulation, which directly sensitizes the body to insulin (19, 20). Administration of recombinant adiponectin to rodents increases the glucose uptake and fat oxidation in muscle, reduces hepatic glucose production, and improves whole body insulin sensitivity (21–23). Adiponectin-deficient (*adipo*(−/−)) mice exhibit insulin resistance and glucose intolerance (24, 25). Previous stud-

* This work was supported by a grant from the Ministry of Education, Culture, Sports, Science and Technology of Japan (for the Translational Systems Biology and Medicine Initiative), Grant-in-Aid for Scientific Research in Priority Areas (A) 16209030 and (A) 18209033 from the Ministry of Education, Culture, Sports, Science, and Technology of Japan (to T. K.). The costs of publication of this article were defrayed in part by the payment of page charges. This article must therefore be hereby marked "*advertisement*" in accordance with 18 U.S.C. Section 1734 solely to indicate this fact.

[1] To whom correspondence should be addressed: Dept. of Diabetes and Metabolic Diseases, Graduate School of Medicine, University of Tokyo, 7-3-1 Hongo, Bunkyo-ku, Tokyo 113-8655, Japan. Tel.: 81-3-5800-8815; Fax: 81-3-5800-9797; E-mail: kadowaki-3im@h.u-tokyo.ac.jp.

ies have shown that adiponectin stimulates fatty acid oxidation in the skeletal muscle and inhibits glucose production in the liver by activating AMP-activated protein kinase (AMPK)[2] (26–29). We also reported that pioglitazone may induce amelioration of insulin resistance and diabetes via an adiponectin-dependent mechanism in the liver and an adiponectin-independent mechanism in the skeletal muscle (30).

Rimonabant has been shown to increase the plasma adiponectin levels in animal models of obesity and diabetes as well as in both diabetic and nondiabetic subjects (15, 31, 32). The results of the RIO-Lipids study provided evidence of a weight loss-independent effect of rimonabant on the plasma adiponectin levels (15). Furthermore, the metabolic improvements induced by rimonabant could be attributed, at least in part, to a moderate but significant increase in the plasma circulating adiponectin levels (15). However, whether the rimonabant-induced increase in the plasma levels of adiponectin might be causally involved in the effects of rimonabant, in particular its insulin-sensitizing effects, has not been addressed experimentally.

To address this issue, in the present study, we used *adipo*(−/−)ob/ob mice (30) to investigate whether rimonabant might be capable of ameliorating insulin resistance in the absence of adiponectin. We found that rimonabant significantly decreased the body weight and food intake to similar degrees in the ob/ob and *adipo*(−/−)ob/ob mice. Furthermore, we found significant amelioration of the insulin resistance in the ob/ob mice, in association with significant up-regulation of the serum adiponectin levels after 21 days of treatment with rimonabant at 30 mg/kg, body weight. The amelioration of insulin resistance in the ob/ob mice was attributed to the decrease of glucose production and activation of AMPK in the liver but not the increased glucose uptake by the skeletal muscle, induced by the drug. Interestingly, insulin resistance was also significantly, although only partially, improved in the *adipo*(−/−)ob/ob mice. Thus, the results suggest that rimonabant ameliorates insulin resistance via both adiponectin-dependent and adiponectin-independent pathways.

EXPERIMENTAL PROCEDURES

Animals and Genotyping—The mice were housed under a 12-h light/dark cycle and fed standard chow, CE-2 (CLEA Japan Inc., Tokyo, Japan). The composition of the chow was as follows: 25.6% (w/w) protein, 3.8% fiber, 6.9% ash, 50.5% carbohydrates, 4% fat, and 9.2% water. Ob/ob and *adipo*(−/−)ob/ob mice were generated by intercrossing *adipo*(+/−)ob/+ mice. All the mice were maintained on a C57Bl/6 background (30). All of the experiments in this study were conducted on 16–20-week-old male littermates. The animal care and experimental procedures were approved by the Animal Care Committee of the University of Tokyo.

Rimonabant Treatment Study—Rimonabant (SR141716) or vehicle (0.1% Tween 80 in saline) was administered to ob/ob and *adipo*(−/−)ob/ob mice at a dose of 30 mg/kg body weight by oral gavage, once daily for 21 consecutive days. Rimonabant was kindly provided by Sanofi-Aventis (Montpellier, France). We measured the body weights and food intake of the mice once daily for 21 consecutive days.

Hyperinsulinemic-Euglycemic Clamp Study—Clamp studies were carried out as described previously (30) with slight modifications. In brief, 2 days before the study, an infusion catheter was inserted into the right jugular vein under general anesthesia induced by sodium pentobarbital. Studies were performed on the mice under conscious and unstressed conditions after 8 h of fasting. A primed continuous infusion of insulin (Humulin R; Lilly) was administered (25.0 milliunits/kg/min), and the blood glucose concentration, monitored every 5 min, was maintained at 100–130 mg/dl by administration of glucose (5 g of glucose/10 ml enriched to ~20% with [6,6-$^2H_2$]glucose (Sigma)) for 120 min. Blood was sampled via tail tip bleeds at 90, 105, and 120 min for determination of the rate of glucose disappearance (R_d). R_d was calculated according to nonsteady-state equations (30), and endogenous glucose production was calculated as the difference between the R_d and the exogenous glucose infusion rate (30).

Western Blot Analysis—Tissues were excised and homogenized in ice-cold buffer A (25 mM Tris-HCl (pH 7.4), 10 mM sodium orthovanadate, 10 mM sodium pyrophosphate, 100 mM sodium fluoride, 10 mM EDTA, 10 mM EGTA, and 1 mM phenylmethylsulfonyl fluoride). The sample buffer for analysis under reducing conditions was composed of 3% SDS, 50 mM Tris-HCl (pH 6.8), 5% 2-mercaptoethanol, and 10% glycerol. Samples were mixed with 5× sample buffer, heated at 95 °C for 5 min for heat denaturation, separated on polyacrylamide gels, and then transferred to a Hybond-P polyvinylidene difluoride transfer membrane (Amersham Biosciences). Bands were detected with ECL detection reagents (Amersham Biosciences). To examine the Akt and AMPK phosphorylation and protein levels, lysates of liver and muscle were analyzed using anti-phospho-Akt (Cell Signaling Technology, Inc., Beverly, MA), anti-Akt (Cell Signaling Technology, Inc.) antibody, anti-phospho-AMPK (Cell Signaling Technology, Inc., Beverly, MA), and anti-AMPK (Cell Signaling Technology, Inc.) antibodies. For the analysis under nonreducing conditions, 2-mercaptoethanol was excluded from the sample buffer described above. To examine the isoforms of adiponectin, the serum samples were diluted 20-fold. Anti-mouse adiponectin antiserum was obtained by immunizing rabbits with the globular domain of mouse recombinant adiponectin produced in *Escherichia coli* (21).

Tissue Sampling for Insulin Signaling Pathway Study—Mice were anesthetized after 16 h of starvation, and 0.05 unit of human insulin (Humulin R; Lilly) was injected into the inferior vena cava. After 5 min, the liver was removed, and the specimens were used for protein extraction as described above.

Plasma Adiponectin and Lipid Measurements—The mice were deprived of access to food for 16 h before the measurements. The plasma adiponectin levels were determined with a mouse adiponectin enzyme-linked immunosorbent assay kit (Otsuka Pharmaceutical Co., Ltd., Tokyo, Japan). Serum triglyceride and free fatty acids (Wako Pure Chemical Industries Ltd., Osaka, Japan) were assayed by enzymatic methods.

[2] The abbreviations used are: AMPK, AMP-activated protein kinase; PEPCK, phosphoenolpyruvate carboxykinase; WAT, white adipose tissue; TG, triglyceride; FFA, free fatty acid; HMW, high molecular weight.

Measurement of Adipocyte Size—Epididymal white adipose tissue and subcutaneous fat were routinely processed for paraffin embedding, and 4-μm sections were cut and mounted on silanized slides. The adipose tissue sections were stained with hematoxylin and eosin, and the total adipocyte area was manually traced and analyzed using the Win ROOF software (Mitani Co. Ltd., Chiba, Japan). The white adipocyte area was measured in 200 or more cells/mouse in each group, in accordance with a previously described method (30), with slight modifications.

Oil Red O Staining and Quantification—Lipid accumulation was assessed by Oil Red O staining in 6-μm frozen sections of the liver fixed in phosphate-buffered 4% paraformaldehyde, according to a previously described method (33) with slight modification. In brief, the livers were washed once for 1 min with H_2O. After an additional wash for 1 min with 60% isopropyl alcohol, the livers were stained for 10 min at 37 °C with freshly diluted Oil Red O solution (6 parts of Oil Red O stock solution and 4 parts of H_2O; the Oil Red O stock solution contained 0.5% Oil Red O in isopropyl alcohol). After one wash for 2 min with 60% isopropyl alcohol and one wash for 1 min with H_2O, the livers were stained for 5 min with hematoxylin. The stain was then washed off with running water, and the silanized slides were stained. Oil Red O staining was quantified on digital images. Color images were acquired with a Nikon digital camera and analyzed using the Image J software. The percentage of the area of Oil Red O staining was measured from 9–10 different sections/mouse in each experimental group. Values were expressed as percentage of area.

Analysis of O_2 Consumption—Oxygen consumption was measured every 3 min for 24 h in the fasting mice using an O_2/CO_2 metabolism measurement device (model MK-5000; Muromachikikai, Tokyo, Japan). After rimonabant treatment for 21 days, each mouse was placed in a sealed chamber (560-ml volume) with an air flow rate of 500 ml/min at room temperature. The amount of oxygen consumed was converted to ml/min by multiplying it with the flow rate.

RNA Preparation and Taqman PCR—Total RNA was extracted from various tissues *in vivo* with TRIzol reagent (Invitrogen), in accordance with the manufacturer's instructions. After treatment with RQ1 RNase-free DNase (Promega, Madison, WI) to remove genomic DNA, cDNA was synthesized with MultiScribe reverse transcriptase (Applied Biosystems, Foster City, CA). Total RNA was prepared from 3T3L1 cells *in vitro* with an RNeasy Mini Kit (Qiagen Co., Düsseldorf, Germany), in accordance with the manufacturer's instructions. mRNA levels were quantitatively analyzed by fluorescence-based reverse transcriptase-PCR. The reverse transcription mixture was amplified with specific primers using an ABI Prism 7000 sequence detector equipped with a thermocycler. The primers used for MCP-1 (monocyte chemoattractant protein-1), resistin, phosphoenolpyruvate carboxykinase (PEPCK), carnitine palmitoyltransferase-1A, the hepatic isoform of carnitine palmitoyltransferase-1, protein phosphatase 2C, and cyclophilin were purchased from Applied Biosystems (Foster City, CA). The relative expression levels were compared by normalization to the expression levels of cyclophilin.

Cell Culture and Differentiation of 3T3L1 Adipocytes and Rimonabant Treatment—3T3L1 preadipocytes were cultured in Dulbecco's modified Eagle's medium containing 25 mM glucose and 10% fetal bovine serum at 37 °C. Confluent cultures were induced to differentiate into adipocytes by incubation in Dulbecco's modified Eagle's medium containing 25 mM glucose, 10% fetal bovine serum, 0.25 units/ml insulin, 0.25 μM dexamethasone, and 0.5 mM isobutyl-1-methylxanthine. After 2 days, the medium was changed to Dulbecco's modified Eagle's medium containing 25 mM glucose, 10% fetal bovine serum, and 0.025 units/ml insulin. All studies were performed on adipocytes 10 days after the initiation of differentiation (Day 0). Rimonabant treatment (100 nM and 1 μM) was started on Day 0, and DMSO was used as the vehicle. Prior to the start of the experiments, the differentiated adipocytes were serum-starved in Dulbecco's modified Eagle's medium containing 25 mM glucose for 16 h at 37 °C.

RESULTS

Absence of Adiponectin Had No Effect on Rimonabant-induced Suppression of Body Weight and Daily Food Intake—The body weight gain was similar between the untreated ob/ob and *adipo*(−/−)ob/ob mice (Fig. 1*A*), as reported previously (30). The food intake was also comparable between the untreated ob/ob and *adipo*(−/−)ob/ob mice (Fig. 1*B*). Rimonabant significantly decreased the body weight and food intake to similar degrees in the ob/ob and *adipo*(−/−)ob/ob mice (Fig. 1, *A* and *B*). After 21 days of rimonabant treatment, both the ob/ob and *adipo*(−/−)ob/ob mice weighed 10% less than the corresponding untreated mice (Fig. 1*A*). Moreover, rimonabant treatment significantly decreased the white adipose tissue (WAT) mass in both subcutaneous and visceral (epididymal, mesenteric, and retroperitoneal) fat to similar degrees in the ob/ob and *adipo*(−/−)ob/ob mice (Fig. 1*C*). To determine whether the presence of adiponectin is required for the reduction of the average adipocyte size induced by rimonabant treatment, we histologically analyzed the epididymal fat pad and subcutaneous WAT after fixation and quantitation of the adipocyte size. The distribution of the adipocyte size in the rimonabant-treated ob/ob and *adipo*(−/−)ob/ob mice was similarly narrowed to that in the untreated ob/ob and *adipo*(−/−)ob/ob mice (Fig. 1, *D* and *E*), and rimonabant treatment significantly reduced the average adipocyte size in the ob/ob and *adipo*(−/−)ob/ob mice to a similar degree (Fig. 1*F*). These findings indicate that the absence of adiponectin had no effect on either the rimonabant-induced decrease of the body weight or the food intake of the mice and that rimonabant treatment can induce a reduction of adipocyte size in the absence of adiponectin or leptin or both.

Rimonabant Increased the Energy Expenditure and Decreased the Serum Triglyceride and Free Fatty Acid Levels to a Similar Degree in the ob/ob and adipo(−/−)ob/ob Mice—In addition to suppressing food intake, rimonabant has been demonstrated to increase the energy expenditure (10, 34), and the increase in energy expenditure has also been shown in CB-1 receptor knock-out mice (35). Since the involvement of adiponectin in this action of rimonabant remains unclear, we investigated the effects of rimonabant on energy expenditure.

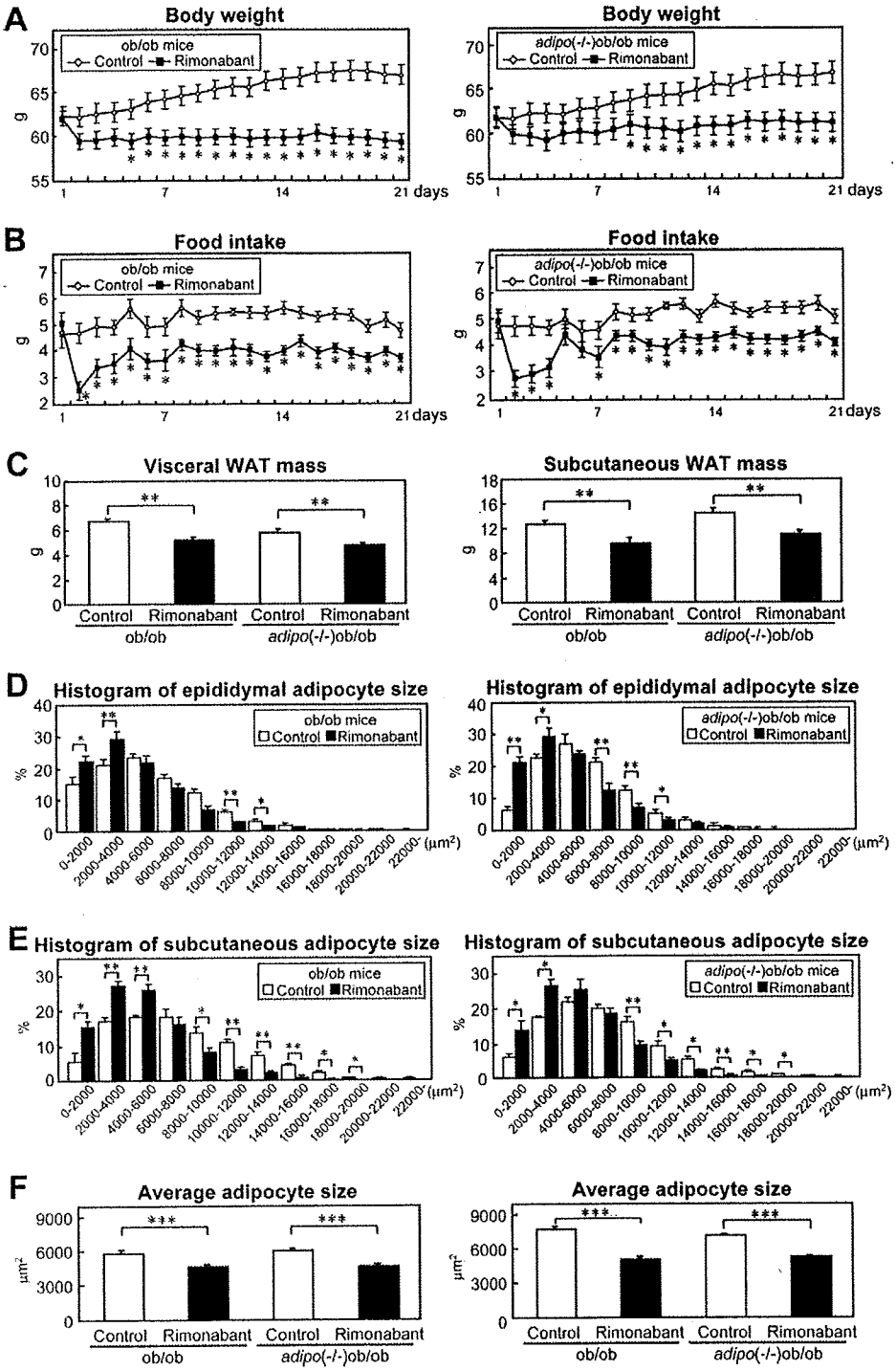

FIGURE 1. **The absence of adiponectin had no effect on rimonabant-induced suppression of body weight and daily food intake.** *A* and *B*, body weights (*A*) and food intake (*B*) of ob/ob (*left panels*) and *adipo*(−/−)ob/ob mice (*right panels*) not treated (*open squares*) and treated (*filled squares*) with rimonabant (n = 12–14/group). Values are means ± S.E. of data obtained from the analysis of ob/ob and *adipo*(−/−)ob/ob mice. *, $p < 0.05$. **, $p < 0.01$. *C*, weight of the total visceral white adipose tissue (*left panel*) and subcutaneous WAT (*right panel*) of ob/ob and *adipo*(−/−)ob/ob mice not treated (*open bars*) and treated (*filled bars*) with rimonabant (n = 9–14/group). Values are means ± S.E. of data obtained from the analysis of ob/ob and *adipo*(−/−)ob/ob mice. **, $p < 0.01$. *D* and *E*, histogram of adipocyte size from epididymal WAT (*D*) and subcutaneous WAT (*E*) of ob/ob (*left panels*) and *adipo*(−/−)ob/ob mice (*right panels*) not treated (*open bars*) and treated (*filled bars*) with rimonabant (n = 5–8/group). Values are means ± S.E. of data obtained from the analysis of ob/ob and *adipo*(−/−)ob/ob mice. *, $p < 0.05$; **, $p < 0.01$. *F*, average size of adipocyte from epididymal WAT (*left panel*) and subcutaneous WAT (*right panel*) of ob/ob and *adipo*(−/−)ob/ob mice not treated (*open bars*) and treated (*filled bars*) with rimonabant (n = 5–8/group). Values are means ± S.E. of data obtained from the analysis of ob/ob and *adipo*(−/−)ob/ob mice. ***, $p < 0.005$.

First, we measured the rectal temperature in the ob/ob and *adipo*(−/−)-ob/ob mice. The temperature was essentially the same (Fig. 2*A*), and rimonabant treatment significantly increased the rectal temperature of the ob/ob and *adipo*(−/−)ob/ob mice to a similar degree (Fig. 2*A*). Second, we investigated the oxygen consumption after 21-day treatment with rimonabant and found that in the dark phase of the daily light cycle, rimonabant increased the energy expenditure to a similar degree in both the ob/ob and *adipo*(−/−)-ob/ob mice (Fig. 2*B*). This effect of rimonabant on the energy expenditure in the ob/ob mice did not require the presence of adiponectin. We next investigated the effects of rimonabant treatment on the serum lipid levels. In addition to reducing the body weight, rimonabant has been demonstrated to reduce the serum triglyceride (TG) (15–18, 32) and free fatty acid (FFA) levels (32). However, the involvement of adiponectin in this action of rimonabant remains unclear. Both the serum TG and FFA levels were indistinguishable between the ob/ob and *adipo*(−/−)ob/ob mice (Fig. 2, *C* and *D*), and rimonabant treatment significantly decreased the levels of both to similar degrees in the ob/ob and *adipo*(−/−)ob/ob mice (Fig. 2, *C* and *D*). This effect of rimonabant on the serum lipids in the ob/ob mice did not require the presence of adiponectin. MCP-1 and resistin have been shown to be important mediators of insulin resistance linked to obesity (36–39). We analyzed the expression of MCP-1 and resistin in the epididymal WAT. The expressions of both MCP-1 and resistin were indistinguishable between the untreated and rimonabant-treated mice of either genotype (Fig. 2, *E* and *F*).

Rimonabant Increased the Plasma Adiponectin Levels in the ob/ob Mice, in Particular of High Molecular Weight Adiponectin—Rimonabant treatment for 21 days significantly increased the plasma adiponectin levels in the ob/ob mice, whereas plasma adiponectin was not detect-

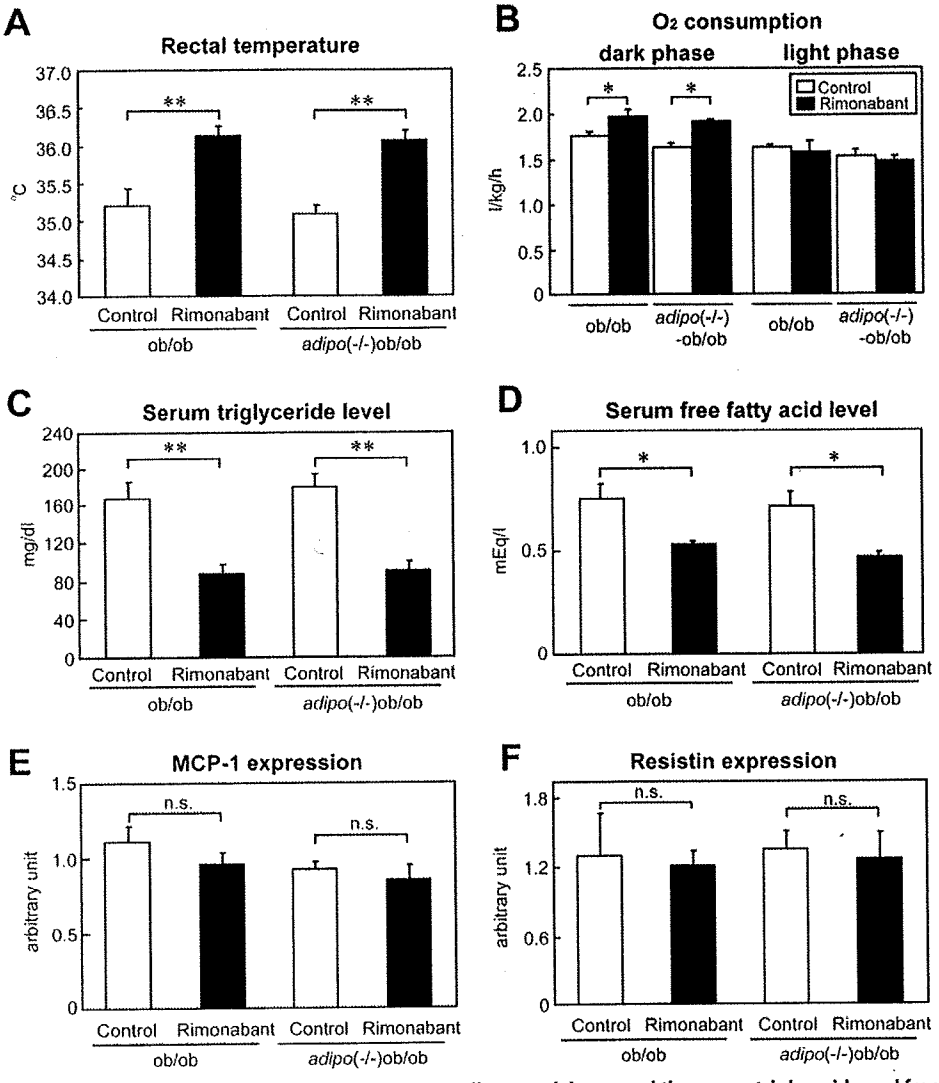

FIGURE 2. **Rimonabant increased the energy expenditure and decreased the serum triglyceride and free fatty acid levels to a similar degree in the ob/ob and *adipo*(−/−)ob/ob mice.** *A* and *B*, rectal temperature (*A*) and O_2 consumption (*B*) in ob/ob and *adipo*(−/−)ob/ob mice not treated (*open bars*) and treated (*filled bars*) with rimonabant (n = 6–10/group). Values are means ± S.E. of data obtained from the analysis of ob/ob mice and *adipo*(−/−)ob/ob mice. *, $p < 0.05$; **, $p < 0.01$. *C* and *D*, serum TG (*C*) and free fatty acid (*FFA*) (*D*) levels in ob/ob and *adipo*(−/−)ob/ob mice not treated (*open bars*) and treated (*filled bars*) with rimonabant. *C*, n = 11–14/group; *D*, n = 4–5/group. Values are means ± S.E. of data obtained from the analysis of ob/ob mice and *adipo*(−/−)ob/ob mice. *, $p < 0.05$. **, $p < 0.01$. *E* and *F*, MCP-1 (*E*) and resistin (*F*) expression levels in the epididymal WAT of ob/ob and *adipo*(−/−)ob/ob mice not treated (*open bars*) and treated (*filled bars*) with rimonabant (n = 7–8/group). Values are means ± S.E. of data obtained from the analysis of ob/ob mice and *adipo*(−/−)ob/ob mice. Values are means ± S.E. *n.s.*, not significant.

able in either the untreated or rimonabant-treated *adipo*(−/−)-ob/ob mice (Fig. 3*A*). High molecular weight (HMW) adiponectin is known to be the most active, and its serum levels have been reported to be decreased in obese individuals and murine models, which is associated with a decrease of the hepatic and muscle AMPK activity and fatty acid combustion and, thereby, exacerbation of insulin resistance (19, 20). Therefore, we analyzed the plasma levels of this isoform of adiponectin by Western blotting. Rimonabant treatment significantly increased the serum levels of HMW adiponectin in the ob/ob mice (Fig. 3*B*). On the other hand, the plasma levels of middle molecular weight and low molecular weight adiponectin were slightly, but not significantly, increased in the rimonabant-treated ob/ob mice (Fig. 3*B*). In regard to the *adipo*(−/−)-ob/ob mice, plasma adiponectin was not detectable in either the untreated or rimonabant-treated mice (Fig. 3*B*). Rimonabant has been reported to increase adiponectin expression and secretion in 3T3F442A adipocyte (6, 40). We next investigated the direct effect of rimonabant on adiponectin secretion using the murine adipocyte cell line 3T3L1 and confirmed that treatment with 100 nM and 1 μM rimonabant actually increased the expression and secretion into the medium of adiponectin (Fig. 3, *C* and *D*).

Rimonabant Improved Hepatic Insulin Resistance in both the ob/ob and adipo(−/−)ob/ob Mice, although the Effect Was Significantly Less Pronounced in the adipo(−/−)-ob/ob Mice—We carried out hyperinsulinemic-euglycemic clamp studies in the ob/ob and *adipo*(−/−)-ob/ob mice to investigate the effect of rimonabant on the insulin resistance in the liver and skeletal muscle. Without rimonabant treatment, the glucose infusion rates were comparable in the ob/ob and *adipo*(−/−)-ob/ob mice (Fig. 4*A*). After 21 days of rimonabant treatment, the glucose infusion rates were significantly increased in both the ob/ob and *adipo*(−/−)ob/ob mice (Fig. 4*A*); however, the increase was significantly less pronounced in the *adipo*(−/−)ob/ob mice. Rimonabant treatment also produced a significant decrease of the endogenous glucose production in both the ob/ob and *adipo*(−/−)ob/ob mice, but the effect was significantly less pronounced in the *adipo*(−/−)ob/ob mice (Fig. 4*B*). The rates of R_d were indistinguishable between the untreated ob/ob and *adipo*(−/−)ob/ob mice, and rimonabant treatment had no effect on this parameter in either genotype (Fig. 4*C*). We next studied the effects on insulin signaling and the downstream reactions in the liver (Fig. 4, *D* and *E*). Insulin-stimulated Akt phosphorylation was significantly increased in rimonabant-treated ob/ob mice as compared with that in the untreated ob/ob mice (Fig. 4*D*), whereas insulin-stimulated Akt phosphorylation only tended to be increased in the rimonabant-treated *adipo*(−/−)ob/ob mice as compared with that in the corresponding untreated mice. The PEPCK expression levels in the liver were comparable in the untreated ob/ob and

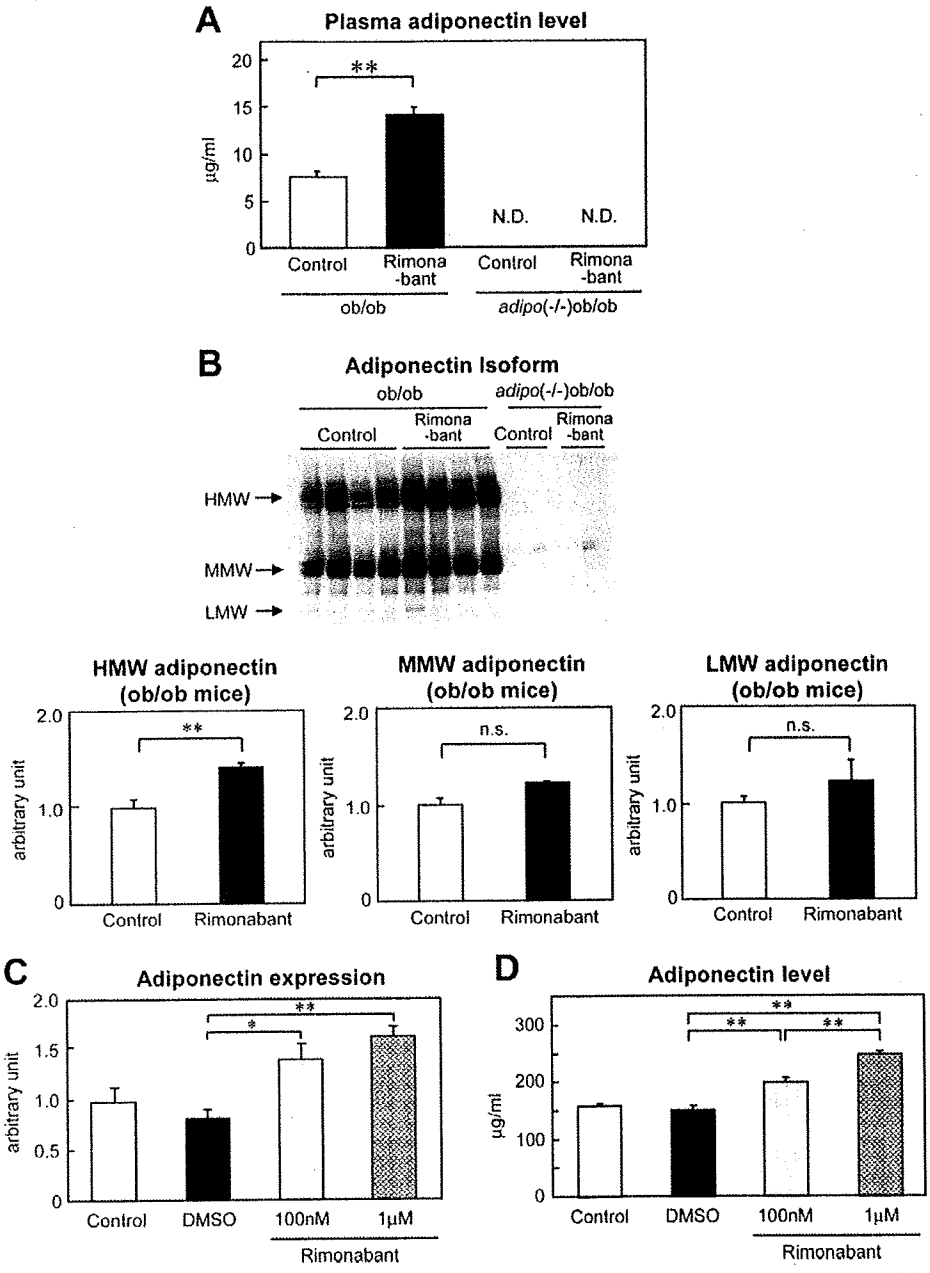

FIGURE 3. **Rimonabant increased the plasma adiponectin levels, in particular of high molecular weight adiponectin, in the ob/ob mice.** *A*, plasma adiponectin levels in ob/ob and *adipo*(−/−)ob/ob mice not treated (*open bar*) and treated (*filled bar*) with rimonabant (n = 7–14/group). Values are means ± S.E. of data obtained from the analysis of ob/ob mice and *adipo*(−/−)ob/ob mice. **, $p < 0.01$. *N.D.*, not detectable. *B*, the different isoforms of plasma adiponectin of ob/ob and *adipo*(−/−)ob/ob mice not treated (*open bars*) and treated (*filled bars*) with rimonabant were analyzed by Western blotting and quantitated by densitometry. The relative ratio of each molecular weight category of adiponectin was normalized to that in the control ob/ob mice not treated with rimonabant (n = 4–8/group). Results are representative of three independent experiments. Values are means ± S.E. of data obtained from the analysis of ob/ob mice and *adipo*(−/−)ob/ob mice. *, $p < 0.05$. *n.s.*, not significant. *C* and *D*, effects of rimonabant on adiponectin mRNA expression (*C*) and adiponectin secretion in the conditioned medium (*D*) of mouse 3T3L1 adipocytes (n = 4–9/group). Shown are controls (*open bars*), DMSO as the vehicle (*filled bars*), 100 nM rimonabant (*gray bars*), and 1 μM rimonabant (*latticed bars*). Values are means ± S.E. of data obtained from the analysis of 3T3L1 adipocytes. *, $p < 0.05$; **, $p < 0.01$.

adipo(−/−)ob/ob mice (Fig. 4*F*). Rimonabant treatment significantly decreased the expression of PEPCK in both the ob/ob and *adipo*(−/−)mice, but the effect was significantly less pronounced in the *adipo*(−/−)ob/ob mice (Fig. 4*F*). These findings indicate that rimonabant ameliorates hepatic but not muscle insulin resistance in mice with an ob/ob background, in both an adiponectin-dependent and adiponectin-independent manner.

Rimonabant Increased the Hepatic AMPK Activities and CPT-1 (Carnitine Palmitoyltransferase-1) Expression Levels in both ob/ob Mice and adipo(−/−)ob/ob Mice, but Its Effect was Significantly Less Pronounced in the adipo(−/−)-ob/ob Mice—We carried out analysis of the liver metabolic activity after the clamp studies to investigate the effect of rimonabant on amelioration of insulin resistance. The AMPK activities were comparable in the untreated ob/ob and *adipo*(−/−)ob/ob mice (Fig. 5*A*). Rimonabant treatment for 21 days increased the AMPK activities in both the ob/ob and *adipo*(−/−)-ob/ob mice, but its effect was significantly less pronounced in the *adipo*(−/−)ob/ob mice (Fig. 5*A*). The expression levels of CPT-1, the rate-limiting enzyme in fatty acid β-oxidation, were also comparable in the untreated ob/ob and *adipo*(−/−)ob/ob mice (Fig. 5*B*). Rimonabant treatment increased the CPT-1 expression in both ob/ob and *adipo*(−/−)ob/ob mice, but its effect was significantly less pronounced in the *adipo*(−/−)ob/ob mice (Fig. 5*B*). The expression levels of protein phosphatase 2C were indistinguishable between the untreated ob/ob and *adipo*(−/−)ob/ob mice, and rimonabant treatment had no effect on the protein phosphatase 2C expression in either genotype (Fig. 5*C*). As reported previously (26, 41), fatty acid oxidation is positively regulated by AMPK in the liver; therefore, we next carried out analysis of the hepatic TG content by Oil Red O staining. The percentage of areas of Oil Red O staining in the liver were comparable in the untreated ob/ob and *adipo*(−/−)ob/ob mice (Fig. 5*D*). Rimonabant treatment significantly decreased the hepatic TG content in both the ob/ob and *adipo*(−/−)mice, but its effect was significantly less pronounced in the *adipo*(−/−)ob/ob mice

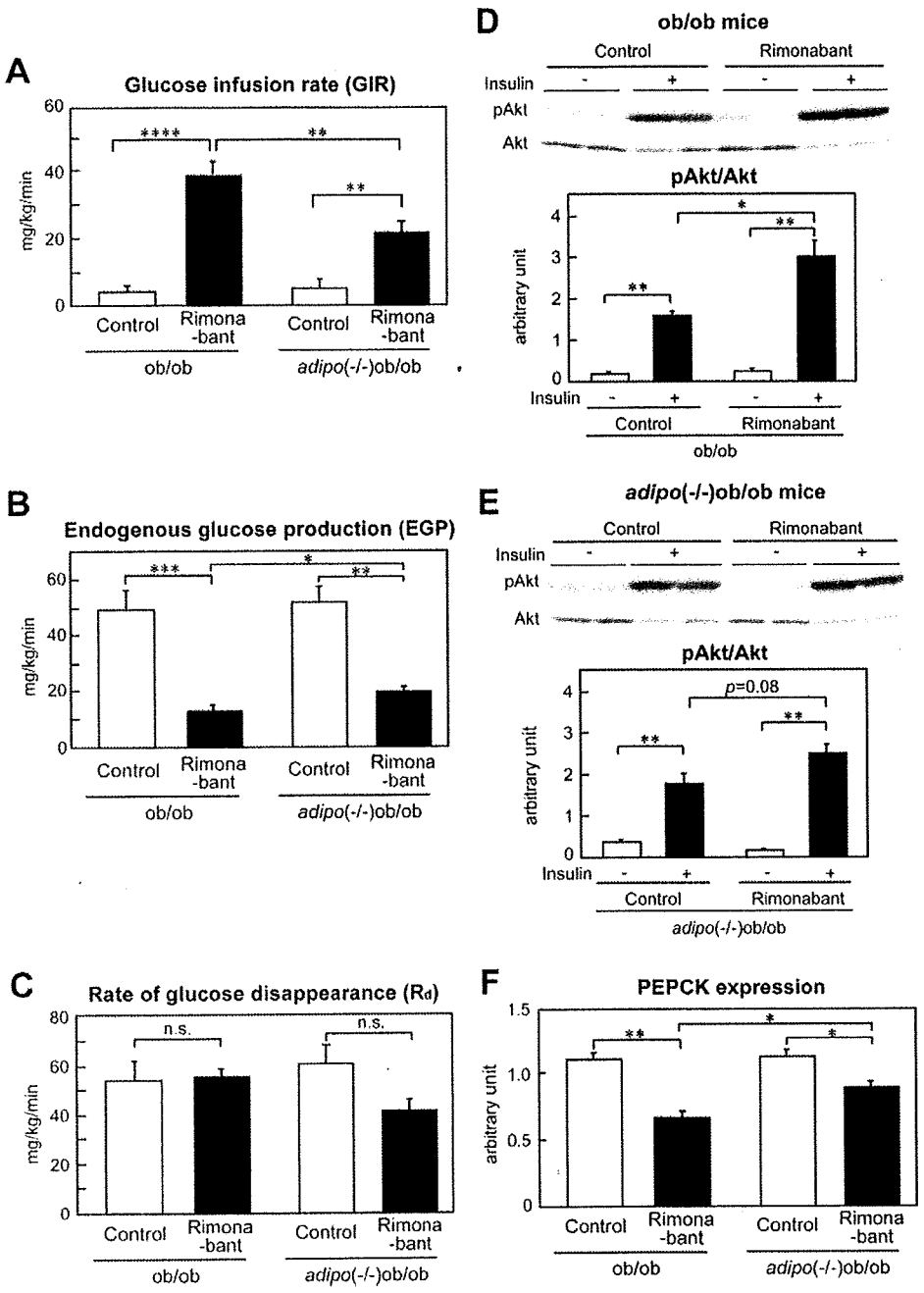

FIGURE 4. **Rimonabant improved hepatic insulin resistance in both ob/ob and *adipo*(−/−)ob/ob mice, although the effect was significantly less pronounced in the *adipo*(−/−)ob/ob mice.** *A–C*, glucose infusion rates (*GIR*) (*A*), endogenous glucose production (*EGP*) (*B*), and rates of glucose disappearance (*Rd*) (*C*) in ob/ob and *adipo*(−/−)ob/ob mice not treated (*open bars*) and treated (*filled bars*) with rimonabant in the clamp study (n = 5–7/group). Values are means ± S.E. of data obtained from the analysis of ob/ob mice and *adipo*(−/−)ob/ob mice. *, $p < 0.05$; **, $p < 0.01$; ***, $p < 0.005$. *D* and *E*, phosphorylations of Akt in the livers of ob/ob (*D*) and *adipo*(−/−)ob/ob mice (*E*) not treated (*open bars*) and treated (*filled bars*) with rimonabant after the injection of insulin (n = 4–5/group). Results are representative of three independent experiments. Values are means ± S.E. of data obtained from the analysis of ob/ob mice and *adipo*(−/−)ob/ob mice. *, $p < 0.05$. *F*, PEPCK expression levels in the livers of ob/ob and *adipo*(−/−)ob/ob mice not treated (*open bars*) and treated (*filled bars*) with rimonabant after the clamp studies (n = 6–7/group). The relative expressions after normalization to the expression level of cyclophilin were compared. Values are means ± S.E. of data obtained from the analysis of ob/ob mice and *adipo*(−/−)ob/ob mice. *, $p < 0.05$; **, $p < 0.01$. pAkt, phospho-Akt. *n.s.*, not significant.

(Fig. 5*D*). We also investigated the AMPK activities in the muscle after the clamp studies. The AMPK activities in the muscle were indistinguishable between the untreated ob/ob and *adipo*(−/−)ob/ob mice, and rimonabant treatment had no effect on the muscle AMPK activity in either genotype (Fig. 5*E*). These findings indicate that rimonabant activates hepatic but not muscle AMPK in mice with an ob/ob background in both an adiponectin-dependent and adiponectin-independent manner.

DISCUSSION

The selective CB-1 blocker rimonabant has been reported to produce weight loss and ameliorate insulin resistance and metabolic abnormalities in obese animals (12, 13), as also in patients with obesity (15–18). Rimonabant has also been reported to increase the plasma adiponectin levels in animal models of obesity and diabetes, as also in diabetic or nondiabetic subjects (15, 31, 32). Adiponectin has been proposed to be a major insulin-sensitizing adipokine (19, 20) and is a plausible candidate as the adipokine mediating the rimonabant-induced amelioration of insulin resistance. Therefore, in this study, we used two obesity models, the ob/ob and *adipo*(−/−)ob/ob mice, to investigate whether the rimonabant-induced increase of plasma adiponectin might be causally involved in the insulin-sensitizing effects of the drug.

Rimonabant treatment decreased the body weight, food intake, and weight of the WAT to similar degrees in the ob/ob and *adipo*(−/−)ob/ob mice. Furthermore, it also increased the energy expenditure and decreased the serum TG and FFA to similar degrees in the ob/ob and *adipo*(−/−)ob/ob mice. Thus, the involvement of adiponectin was not requited for rimonabant to exert its effects.

Significant improvement of the insulin resistance was observed in the ob/ob mice following rimonabant treatment, in association with significant up-regulation of the plasma adiponectin levels, in particular of HMW. Amelioration of insulin resistance in the ob/ob mice was considered to be attributable to improvement of the hepatic but not muscle insulin resistance. Interestingly, these

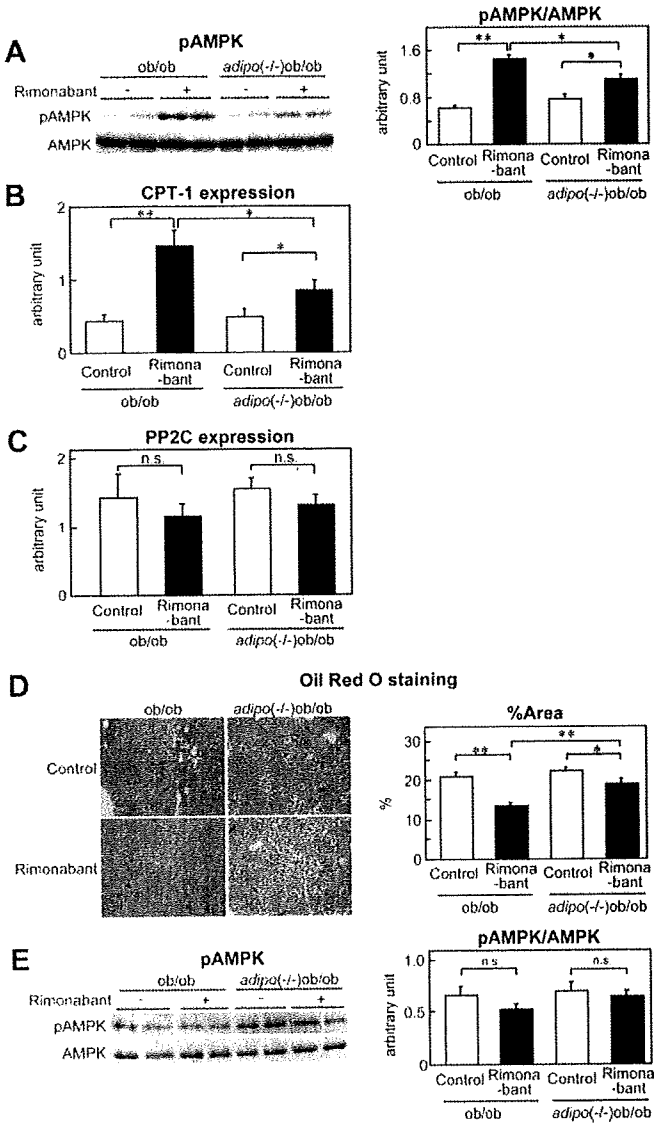

FIGURE 5. **Rimonabant increased the hepatic AMPK activities and CPT-1 expression levels in both ob/ob mice and *adipo*(−/−)ob/ob mice, but the effects were significantly less pronounced in the *adipo*(−/−)ob/ob mice.** *A*, phosphorylations of AMPK in the livers of ob/ob and *adipo*(−/−)ob/ob mice not treated (*open bars*) and treated (*filled bars*) with rimonabant after the clamp studies (n = 4–5/group). Results are representative of three independent experiments. Values are means ± S.E. of data obtained from the analysis of ob/ob mice and *adipo*(−/−)ob/ob mice. *, $p < 0.05$; **, $p < 0.01$. *B* and *C*, carnitine palmitoyltransferase-1 (*CPT-1*) (B) and protein phosphatase 2C (*PP2C*) (*C*) expression levels in the liver of ob/ob and *adipo*(−/−)ob/ob mice not treated (*open bars*) and treated (*filled bars*) with rimonabant after the clamp studies (n = 4–9/group). Relative expressions after normalization to the expression level of cyclophilin were compared. Values are means ± S.E. of data obtained from the analysis of ob/ob mice and *adipo*(−/−)ob/ob mice. *, $p < 0.05$; **, $p < 0.01$. *D*, Oil Red O staining in the livers of ob/ob and *adipo*(−/−)ob/ob mice not treated (*open bars*) and treated (*filled bars*) with rimonabant (n = 6–10/group). Representative liver histology as viewed on a computer monitor is shown. Original magnification, ×100. Values are means ± S.E. of data obtained from the analysis of ob/ob mice and *adipo*(−/−)ob/ob mice. *, $p < 0.05$; **, $p < 0.01$. *E*, phosphorylation levels of AMPK in the muscle of ob/ob and *adipo*(−/−)ob/ob mice not treated (*open bars*) and treated (*filled bars*) with rimonabant after the clamp studies (n = 5/group). Results are representative of three independent experiments. Values are means ± S.E. pAMPK, phospho-AMPK; *n.s.*, not significant.

improvements induced by rimonabant were significantly less pronounced in the *adipo*(−/−)ob/ob mice, indicating that adiponectin is involved in the rimonabant-mediated amelioration of hepatic insulin resistance. In fact, although a significant decrease of the PEPCK expression levels was observed, the AMPK activity was significantly increased, and the hepatic TG content was decreased in the ob/ob mice; all of these changes were significantly less pronounced in the *adipo*(−/−)ob/ob mice lacking adiponectin. We reported from a previous study that adiponectin, especially HMW adiponectin, stimulates AMPK activation in the liver (26, 42). These findings suggest that rimonabant treatment activates AMPK in the liver via increasing the secretion of HMW adiponectin and then decreases the expression of PEPCK to inhibit glucose production and increase CPT-1 expression, thereby stimulating fatty acid oxidation in the liver.

On the other hand, rimonabant treatment also produced significant amelioration of hepatic insulin resistance in the absence of adiponectin. This amelioration was possibly attributable to the reduction of body weight (Fig. 1*A*) but not to suppression of MCP-1 and resistin expression (Fig. 2, *E* and *F*). Alternatively, this amelioration was possibly due to the direct activation of AMPK by rimonabant in the liver. In fact, recent reports have shown that AMPK activity was significantly higher in the liver of hepatocyte-specific CB-1 receptor knock-out mice, although the serum adiponectin levels in these animals remained unchanged (35, 43), suggesting that rimonabant treatment directly activates hepatic AMPK, even without the mediation of adiponectin, and decreases the expression of PEPCK to inhibit glucose production in the liver.

In addition, Osei-Hyiaman *et al.* (35) have reported that CPT-1 activity in the liver was significantly increased when systemic CB-1 receptors were blocked pharmacologically in wild-type mice. Moreover, hepatic CPT-1 activity increased, and hepatic TG content decreased when hepatic CB-1 receptors were blocked genetically (35). These data suggest that CB-1 receptor blockade stimulates CPT-1 activity and increases fatty acid combustion to decrease the TG content in the liver. Consistent with this, rimonabant actually increased CPT-1 expression and decreased the TG content in the livers of ob/ob and *adipo*(−/−)ob/ob mice. However, these effects were markedly attenuated in the *adipo*(−/−)ob/ob mice, suggesting that increased CPT-1 expression and decreased hepatic TG content by rimonabant were also mediated by adiponectin-dependent as well as adiponectin-independent pathways.

Based on our findings, we propose that there are two distinct pathways by which rimonabant ameliorates insulin resistance, one an adiponectin-dependent pathway and the other an adiponectin-independent pathway (Fig. 6). Rimonabant increases the plasma levels of adiponectin, in particular of HMW adiponectin, which induces AMPK activation and decreases gluconeogenesis in the liver, thereby ameliorating insulin resistance. On the other hand, in a manner independent of adiponectin, rimonabant directly induces AMPK activation and decreases gluconeogenesis in the liver, possibly via the hepatic CB-1 receptor (35, 43), which also contributes to ameliorating insulin resistance. In addition, rimonabant decreases food intake and increases energy expenditure, which are related to reduction of body weight. This body weight loss may be also associated with ameliorating insulin resistance via adiponectin-dependent and adiponectin-independent pathways (Fig. 6).

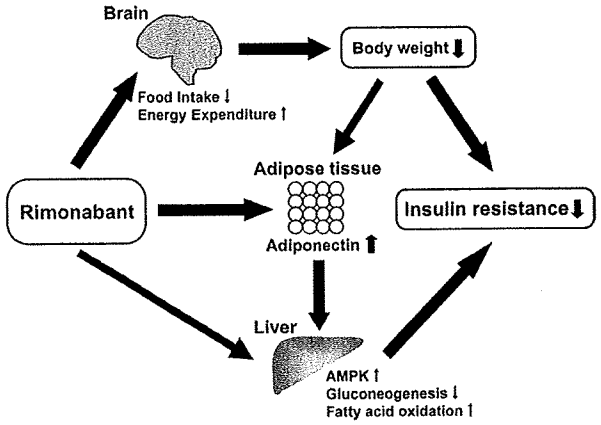

FIGURE 6. **Rimonabant ameliorates insulin resistance via both adiponectin-dependent and adiponectin-independent pathways.** There are two distinct pathways by which rimonabant ameliorates insulin resistance, one an adiponectin-dependent pathway and the other an adiponectin-independent pathway. Rimonabant increases the plasma levels of adiponectin, in particular of HMW adiponectin, which induces AMPK activation and decreases gluconeogenesis in the liver, thereby ameliorating insulin resistance. On the other hand, in a manner independent of adiponectin, rimonabant directly induces AMPK activation and decreases gluconeogenesis in the liver, possibly via hepatic CB-1 receptor, which also contributes to ameliorating insulin resistance. In addition, rimonabant decreases food intake and increases energy expenditure, which are related to reduction of body weight. This body weight loss may be also associated with ameliorating insulin resistance via adiponectin-dependent and adiponectin-independent pathways.

Rimonabant is metabolized in the liver by cytochrome P-450 CYP3A4 and amidohydrolase and excreted into the bile (44, 45). The oral bioavailability of rimonabant is low to moderate; this is due to the extensive first pass metabolism of the drug (European Medicines Agency). Therefore, in this study, the concentration in the liver of the orally administered rimonabant might be higher than that in other tissues, such as the muscle, because of the first pass effect of the liver. Although intraperitoneally administered rimonabant was reported in a previous study to significantly increase the glucose uptake in the soleus muscle of ob/ob mice (10), no improvement of the insulin resistance in the muscle was observed in our study. One of the reasons for this difference may be the lower concentration of rimonabant in the muscle due to the first pass effect of the liver.

In the four double-blind trials (RIO-Lipids (15), RIO-Europe (16), RIO-North America (17), and RIO-Diabetes (18)) the most frequent adverse events among individuals treated with rimonabant were nausea, dizziness, diarrhea, and insomnia, each occurring at a 1–9% greater frequency than that in the placebo group. In the RIO-Lipids, RIO-Europe, and RIO-North America, the drug had to be discontinued due to the development of psychiatric disorders (mainly depression) in 6–7% of rimonabant-treated individuals, an absolute increase of 2–5% over the frequency in the placebo group (44). Substance dependence with rimonabant has not been reported. The absence of the appearance of clinical signs in toxicology studies with a recovery period indicates that rimonabant does not possess the potential to produce withdrawal syndrome (European Medicines Agency).

Many reports have shown the efficacy of cannabinoid agonists in chronic pain (46). In a rodent model of inflammatory pain, anandamide, one of the endogenous cannabinoids, suppressed the development and maintenance of thermal hyperalgesia (47). This analgesic effect was diminished by concurrent administration of the CB-1 antagonist, rimonabant, and anandamide. Although rimonabant alters the sensitivity to pain (47), it does not necessarily induce pain itself. On the contrary, rimonabant has recently been shown to prevent indomethacin-induced intestinal injury by decreasing the levels of the proinflammatory cytokine, tumor necrosis factor α, in rodents (48), indicating its potential anti-inflammatory activity in acute and chronic diseases. In neurogenic inflammatory pain, including arthritis and neuropathy, many cytokines, especially tumor necrosis factor α, play a key role in the generation and maintenance of hyperalgesia (49). On the basis of these findings, Costa (50) indicated that the anti-tumor necrosis factor α effect of rimonabant might contribute to its anti-inflammatory activity and consequently to the relief of pain. However, further investigation and accumulation of further evidence on the effect of rimonabant on pain are needed. At least, in the four clinical trials mentioned above, side effects associated with pain, such as hyperalgesia or hypoalgesia, were not reported. Furthermore, it has been suggested that although females might perceive pain differently from males (51, 52), the anti-obesity effects of rimonabant appeared to be similar in males and females (European Medicines Agency).

In conclusion, this study demonstrated for the first time that rimonabant ameliorates insulin resistance via both adiponectin-dependent and adiponectin-independent pathways.

Acknowledgments—We thank Ritsuko Hoshino, Katsuyoshi Kumagai, Sayaka Sasamoto, Kayo Nishitani, Naniko Kasuga, and Hiroshi Chiyonobu for excellent technical assistance and animal care.

REFERENCES

1. Flier, J. S. (2004) *Cell* **116,** 337–350
2. Friedman, J. M. (2000) *Nature* **404,** 632–634
3. Reaven, G. M. (1988) *Diabetes* **37,** 1595–1607
4. Di Marzo, V., Goparaju, S. K., Wang, L., Liu, J., Bátkai, S., Járai, Z., Fezza, F., Miura, G. I., Palmiter, R. D., Sugiura, T., and Kunos, G. (2001) *Nature* **410,** 822–825
5. Cota, D., Marsicano, G., Tschöp, M., Grübler, Y., Flachskamm, C., Schubert, M., Auer, D., Yassouridis, A., Thöne-Reineke, C., Ortmann, S., Tomassoni, F., Cervino, C., Nisoli, E., Linthorst, A. C. E., Pasquali, R., Lutz, B., Stalla, G. K., and Pagotto, U. (2003) *J. Clin. Invest.* **112,** 423–431
6. Bensaid, M., Gary-Bobo, M., Esclangon, A., Maffrand, J. P., Le Fur, G., Oury-Donat, F., and Soubrié, P. (2003) *Mol. Pharmacol.* **63,** 908–914
7. Di Marzo, V., Bifulco, M., and De Petrocellis, L. (2004) *Nat. Rev. Drug Discov.* **3,** 771–784
8. Howlett, A. C., Breivogel, C. S., Childers, S. R., Deadwyler, S. A., Hampson, R. E., and Porrino, L. J. (2004) *Neuropharmacology* **47,** Suppl. 1, 345–358
9. Osei-Hyiaman, D., DePetrillo, M., Pacher, P., Liu, J., Radaeva, S., Bátkai, S., Harvey-White, J., Mackie, K., Offertáler, L., Wang, L., and Kunos, G. (2005) *J. Clin. Invest.* **115,** 1298–1305
10. Liu, Y. L., Connoley, I. P., Wilson, C. A., and Stock, M. J. (2005) *Int. J. Obes. Relat. Metab. Disord.* **29,** 183–187
11. Kola, B., Hubina, E., Tucci, S. A., Kirkham, T. C., Garcia, E. A., Mitchell, S. E., Williams, L. M., Hawley, S. A., Hardie, D. G., Grossman, A. B., and Korbonits, M. (2005) *J. Biol. Chem.* **280,** 25196–25201
12. Ravinet Trillou, C., Arnone, M., Delgorge, C., Gonalons, N., Keane, P., Maffrand, J. P., and Soubrié, P. (2003) *Am. J. Physiol.* **284,** R345–R353
13. Cota, D., Marsicano, G., Lutz, B., Vicennati, V., Stalla, G. K., Pasquali, R.,

and Pagotto, U. (2003) *Int. J. Obes. Relat. Metab. Disord.* **27,** 289–301
14. Matias, I., Gonthier, M. P., Orlando, P., Martiadis, V., De Petrocellis, L., Cervino, C., Petrosino, S., Hoareau, L., Festy, F., Pasquali, R., Roche, R., Maj, M., Pagotto, U., Monteleone, P., and Di Marzo, V. (2006) *J. Clin. Endocrinol. Metab.* **91,** 3171–3180
15. Després, J. P., Golay, A., and Sjöström, L. (2005) *N. Engl. J. Med.* **353,** 2121–2134
16. Van Gaal, L. F., Rissanen, A. M., Scheen, A. J., Ziegler, O., and Rössner, S. (2005) *Lancet* **365,** 1389–1397
17. Pi-Sunyer, F. X., Aronne, L. J., Heshmati, H. M., Devin, and Rosenstock, J. (2006) *J. Am. Med. Assoc.* **295,** 761–775
18. Scheen, A. J., Finer, N., Hollander, P., Jensen, M. D., and Van Gaal, L. F. (2006) *Lancet* **368,** 1660–1672
19. Kadowaki, T., Yamauchi, T., Kubota, N., Hara, K., Ueki, K., and Tobe, K. (2006) *J. Clin. Invest.* **116,** 1784–1792
20. Scherer, P. E. (2006) *Diabetes* **55,** 1537–1545
21. Yamauchi, T., Kamon, J., Waki, H., Terauchi, Y., Kubota, N., Hara, K., Mori, Y., Ide, T., Murakami, K., Tsuboyama-Kasaoka, N., Ezaki, O., Akanuma, Y., Gavrilova, O., Vinson, C., Reitman, M. L., Kagechika, H., Shudo, K., Yoda, M., Nakano, Y., Tobe, K., Nagai, R., Kimura, S., Tomita, M., Froguel, P., and Kadowaki, T. (2001) *Nat. Med.* **7,** 941–946
22. Berg, A. H., Combs, T. P., Du, X., Brownlee, M., and Scherer, P. E. (2001) *Nat. Med.* **7,** 947–953
23. Fruebis, J., Tsao, T. S., Javorschi, S., Ebbets-Reed, D., Erickson, M. R., Yen, F. T., Bihain, B. E., and Lodish, H. F. (2001) *Proc. Natl. Acad. Sci. U. S. A* **98,** 2005–2010
24. Kubota, N., Terauchi, Y., Yamauchi, T., Kubota, T., Moroi, M., Matsui, J., Eto, K., Yamashita, T., Kamon, J., Satoh, H., Yano, W., Froguel, P., Nagai, R., Kimura, S., Kadowaki, T., and Noda, T. (2002) *J. Biol. Chem.* **277,** 25863–25866
25. Nawrocki, A. R., Rajala, M. W., Tomas, E., Pajvani, U. B., Saha, A. K., Trumbauer, M. E., Pang, Z., Chen, A. S., Ruderman, N. B., Chen, H., Rossetti, L., and Scherer, P. E. (2006) *J. Biol. Chem.* **281,** 2654–2660
26. Yamauchi, T., Kamon, J., Minokoshi, Y., Ito, Y., Waki, H., Uchida, S., Yamashita, S., Noda, M., Kita, S., Ueki, K., Eto, K., Akanuma, Y., Froguel, P., Foufelle, F., Ferre, P., Carling, D., Kimura, S., Nagai, R., Kahn, B. B., and Kadowaki, T. (2002) *Nat. Med.* **8,** 1288–1295
27. Tomas, E., Tsao, T. S., Saha, A. K., Murrey, H. E., Zhang, Cc. C., Itani, S. I., Lodish, H. F., and Ruderman, N. B. (2002) *Proc. Natl. Acad. Sci. U. S. A* **99,** 16309–16313
28. Kemp, B. E., Stapleton, D., Campbell, D. J., Chen, Z. P., Murthy, S., Walter, M., Gupta, A., Adams, J. J., Katsis, F., van Denderen, B., Jennings, I. G., Iseli, T., Michell, B. J., and Witters, L. A. (2003) *Biochem. Soc. Trans.* **31,** 162–168
29. Hardie, D. G. (2004) *J. Cell Sci.* **117,** 5479–5487
30. Kubota, N., Terauchi, Y., Kubota, T., Kumagai, H., Itoh, S., Satoh, H., Yano, W., Ogata, H., Tokuyama, K., Takamoto, I., Mineyama, T., Ishikawa, M., Moroi, M., Sugi, S., Yamauchi, T., Ueki, K., Tobe, K., Noda, T., Nagai, R., and Kadowaki, T. (2006) *J. Biol. Chem.* **281,** 8748–8755
31. Poirier, B., Bidouard, J. P., Cadrouvele, C., Marniquet, X., Staels, B., O'Connor, S. E., Janiak, P., and Herbert, J. M. (2005) *Diabetes Obes. Metab.* **7,** 65–72
32. Gary-Bobo, M., Elachouri, G., Gallas, J. F., Janiak, P., Marini, P., Ravinet-Trillou, C., Chabbert, M., Cruccioli, N., Pfersdorff, C., Roque, C., Arnone, M., Croci, T., Soubrié, P., Oury-Donat, F., Maffrand, J. P., Scatton, B., Lacheretz, F., Le Fur, G., Herbert, J. M., and Bensaid, M. (2007) *Hepatology* **46,** 122–129
33. Kubota, N., Terauchi, Y., Miki, H., Tamemoto, H., Yamauchi, T., Komeda, K., Nakano, R., Ishii, C., Sugiyama, T., Eto, K., Tsubamoto, Y., Okuno, A., Murakami, K., Sekihara, H., Hasegawa, G., Naito, M., Toyoshima, Y., Tanaka, S., Shiota, K., Kitamura, T., Fujita, T., Ezaki, O., Aizawa, S., Nagai, R., Tobe, K., Kimura, S., and Kadowaki, T. (1999) *Mol. Cell* **4,** 597–609
34. Addy, C., Wright, H., Van Laere, K., Gantz, I., Erondu, N., Musser, B. J., Lu, K., Yuan, J., Sanabria-Bohórquez, S. M., Stoch, A., Stevens, C., Fong, T. M., De Lepeleire, I., Cilissen, C., Cote, J., Rosko, K., Gendrano, I. N., III, Nguyen, A. M., Gumbiner, B., Rothenberg, P., de Hoon, J., Bormans, G., Depré, M., Eng, W. S., Ravussin, E., Klein, S., Blundell, J., Herman, G. A., Burns, H. D., Hargreaves, R. J., Wagner, J., Gottesdiener, K., Amatruda, J. M., and Heymsfield, S. B. (2008) *Cell Metab.* **7,** 68–78
35. Osei-Hyiaman, D., Liu, J., Zhou, L., Godlewski, G., Harvey-White, J., Jeong, W., Batkai, S., Marsicano, G., Lutz, B., Buettner, C., and Kunos, G. (2008) *J. Clin. Invest.* **118,** 3160–3169
36. Kamei, N., Tobe, K., Suzuki, R., Ohsugi, M., Watanabe, T., Kubota, N., Ohtsuka-Kowatari, N., Kumagai, K., Sakamoto, K., Kobayashi, M., Yamauchi, T., Ueki, K., Oishi, Y., Nishimura, S., Manabe, I., Hashimoto, H., Ohnishi, Y., Ogata, H., Tokuyama, K., Tsunoda, M., Ide, T., Murakami, K., Nagai, R., and Kadowaki, T. (2006) *J. Biol. Chem.* **281,** 26602–26614
37. Steppan, C. M., Bailey, S. T., Bhat, S., Brown, E. J., Banerjee, R. R., Wright, C. M., Patel, H. R., Ahima, R. S., and Lazar, M. A. (2001) *Nature* **409,** 307–312
38. Kershaw, E. E., and Flier, J. S. (2004) *J. Clin. Endocrinol. Metab.* **89,** 2548–2556
39. Kanda, H., Tateya, S., Tamori, Y., Kotani, K., Hiasa, K., Kitazawa, R., Kitazawa, S., Miyachi, H., Maeda, S., Egashira, K., and Kasuga, M. (2006) *J. Clin. Invest.* **116,** 1494–1505
40. Gary-Bobo, M., Elachouri, G., Scatton, B., Le Fur, G., Oury-Donat, F., and Bensaid, M. (2006) *Mol. Pharmacol.* **69,** 471–478
41. Muoio, D. M., Seefeld, K., Witters, L. A., and Coleman, R. A. (1999) *Biochem. J.* **338,** 783–791
42. Hada, Y., Yamauchi, T., Waki, H., Tsuchida, A., Hara, K., Yago, H., Miyazaki, O., Ebinuma, H., and Kadowaki, T. (2007) *Biochem. Biophys. Res. Commun.* **356,** 487–493
43. Jeong, W., Osei-Hyiaman, D., Park, O., Liu, J., Bátkai, S., Mukhopadhyay, P., Horiguchi, N., Harvey-White, J., Marsicano, G., Lutz, B., Gao, B., and Kunos, G. (2008) *Cell Metab.* **7,** 227–235
44. Padwal, R. S., and Majumdar, S. R. (2007) *Lancet* **369,** 71–77
45. Xie, S., Furjanic, M. A., Ferrara, J. J., McAndrew, N. R., Ardino, E. I., Ngondara, A., Bernstein, Y., Thomas, K. J., Kim, E., Walker, J. M., Nagar, S., Ward, S. J., and Raffa, R. B. (2007) *J. Clin. Pharm. Ther.* **32,** 209–231
46. Hosking, R. D., and Zajicek, J. P. (2008) *Br. J. Anaesth.* **101,** 59–68
47. Richardson, I. D., Kilo, S., and Hargreaves, K. M. (1998) *Pain* **75,** 111–119
48. Croci, T., Landi, M., Galzin, A. M., and Marini, P. (2003) *Br. J. Phamacol.* **140,** 115–122
49. Schäfers, M., Geis, C., Svensson, C. I., Luo, Z. D., and Sommer, C. (2003) *Eur. J. Neurosci.* **17,** 791–804
50. Costa, B. (2007) *Br. J. Pharmacol.* **150,** 535–537
51. Hurley, R. W., and Adams, M. C. (2008) *Anesth. Analg.* **170,** 309–317
52. Chin, M. L., and Rosenquist, R. (2008) *Anesth. Analg.* **170,** 4–5

THE JOURNAL OF BIOLOGICAL CHEMISTRY VOL. 284, NO. 8, pp. 5050–5055, February 20, 2009

The Death Effector Domain-containing DEDD Supports S6K1 Activity via Preventing Cdk1-dependent Inhibitory Phosphorylation*

Received for publication, November 12, 2008, and in revised form, December 22, 2008 Published, JBC Papers in Press, December 22, 2008, DOI 10.1074/jbc.M808598200

Nobuya Kurabe[‡], Satoko Arai[‡], Akemi Nishijima[‡], Naoto Kubota[§], Futoshi Suizu[¶], Mayumi Mori[‡], Jun Kurokawa[‡], Miki Kondo-Miyazaki[‡], Tomohiro Ide[‖], Kouji Murakami[‖], Katsuhisa Miyake[**], Kohjiro Ueki[§], Hisashi Koga[‡‡], Yutaka Yatomi[§], Fumio Tashiro[§§], Masayuki Noguchi[¶], Takashi Kadowaki[§], and Toru Miyazaki[‡1]

From the [‡]Division of Molecular Biomedicine for Pathogenesis, Center for Disease Biology and Integrative Medicine, and the [§]Department of Internal Medicine, Faculty of Medicine, University of Tokyo, Tokyo 113-0033, Japan, the [¶]Division of Cancer Biology, Institute for Genetic Medicine, Hokkaido University, Hokkaido, 060-0815, Japan, [‖]Bioscience Division I, Metabolic Discovery Research Laboratories, Kyorin Pharmaceutical Company Ltd., Tochigi 329-0114, Japan, the [**]Division of Nephrology and Rheumatology, Department of Internal Medicine, Fukuoka University School of Medicine, Fukuoka 812-8581, Japan, the [‡‡]Department of Human Genome Research, Kazusa DNA Research Institute, Kisarazu, Chiba 292-0818, Japan, and the [§§]Department of Biological Science and Technology, Faculty of Industrial Science and Technology, Tokyo University of Science, Noda, Chiba 278-8510, Japan

Cell cycle regulation and biochemical responses upon nutrients and growth factors are the major regulatory mechanisms for cell sizing in mammals. Recently, we identified that the death effector domain-containing DEDD impedes mitotic progression by inhibiting Cdk1 (cyclin-dependent kinase 1) and thus maintains an increase of cell size during the mitotic phase. Here we found that DEDD also associates with S6 kinase 1 (S6K1), downstream of phosphatidylinositol 3-kinase, and supports its activity by preventing inhibitory phosphorylation of S6K1 brought about by Cdk1 during the mitotic phase. DEDD$^{-/-}$ cells showed reduced S6K1 activity, consistently demonstrating decreased levels in activating phosphorylation at the Thr-389 site. In addition, levels of Cdk1-dependent inhibitory phosphorylation at the C terminus of S6K1 were enhanced in DEDD$^{-/-}$ cells and tissues. Consequently, as in S6K1$^{-/-}$ mice, the insulin mass within pancreatic islets was reduced in DEDD$^{-/-}$ mice, resulting in glucose intolerance. These findings suggest a novel cell sizing mechanism achieved by DEDD through the maintenance of S6K1 activity prior to cell division. Our results also suggest that DEDD may harbor important roles in glucose homeostasis and that its deficiency might be involved in the pathogenesis of type 2 diabetes mellitus.

Cell size is closely related to specialized cell function and to the specific patterning of tissues in the body. Cell sizing is regulated mainly by two mechanisms: cell cycle control and the biochemical response to nutrients and/or growth factors (1–5). During cell cycle progression, both the G_1 (which is believed to be dominant) and the G_2 periods are important for cells to increase their volume (6–9). In addition, we recently provided evidence that the mitotic period (M phase) also influences cell size, through analysis of DEDD-deficient mice (10, 11). The DEDD molecule was initially described as a member of the death effector domain (DED)[2]-containing protein family (12). Although the absence of DEDD did not apparently influence progression of apoptosis (10), we found that during mitosis, DEDD is associated with Cdk1-cyclin B1 and that it decreases the kinase activity of Cdk1. This response impedes the Cdk1-dependent mitotic program to shut off synthesis of ribosomal RNA (rRNA) and protein and is consequently useful in gaining sufficient cell growth prior to cell division. Depletion of DEDD consistently results in a shortened mitotic duration and an overall reduction in the amount of cellular rRNA and protein and, furthermore, in cell and body size (10, 11).

Of the biochemical responses responsible for cell sizing, the signaling cascade involving phosphatydilinositol 3-kinase (PI3K) and its downstream target of rapamycin (TOR) is most crucial (13–15). In mammals, upon stimulation by growth factors, including insulin, the mammalian TOR (mTOR) cooperates with PI3K-dependent effectors to activate S6K1, thereby phosphorylating the 40 S ribosomal protein S6, and subsequently enhances translation of the 5′-terminal oligopyrimidine sequences that encode components of the translational machinery. This reaction increases the number of ribosomes and the efficacy of protein synthesis, thus critically promoting cell growth (16–18). Therefore, mice deficient for S6K1 (S6K1$^{-/-}$) had reduced cell and body size (19–23). This effect also involves S6K1 in maintenance of glucose tolerance. S6K1

* This work was supported, in whole or in part, by National Institutes of Health Grant 5RO1AI50948-05. This work was also supported by grants-in-aid from the Ministry of Education, Sports, Culture, Science, and Technology, Japan, the Takeda Science Foundation (to T. M. and S. A.), the Mitsubishi Pharma Research Foundation, the Mochida Memorial Foundation for Medical and Pharmaceutical Research, the Danone Institute of Nutrition for Health, the Uehara Memorial Foundation (to T. M.), the Kanae Foundation for the Promotion of Medical Science, and the Kanzawa Medical Research Foundation (to S. A.). The costs of publication of this article were defrayed in part by the payment of page charges. This article must therefore be hereby marked "*advertisement*" in accordance with 18 U.S.C. Section 1734 solely to indicate this fact.

[1] To whom correspondence should be addressed: 7-3-1 Hongo, Bunkyo-ku, Tokyo 113-0033, Japan. Tel.: 81-3-5841-1435; Fax: 81-3-5841-1438; E-mail: tm@m.u-tokyo.ac.jp.

[2] The abbreviations used are: DED, death effector domain; rRNA, ribosomal RNA; S6K1, S6 kinase 1; PI3K, phosphatidylinositol 3-kinase; TOR, target of rapamycin; mTOR, mammalian TOR; MEF, mouse embryonic fibroblast; siRNA, small interfering RNA; GST, glutathione *S*-transferase; rpS6, S6 ribosomal protein.

significantly supports the size of insulin-producing β cells within pancreatic Langerhans islets (24, 25). Thus, in S6K1$^{-/-}$ mice, the insulin mass was diminished, which resulted in ineffective secretion of insulin upon glucose administration (21, 23).

The activation of S6K1 proceeds through chronological phosphorylation at various residues, toward the crucial phosphorylation of Thr-389, present within the linker domain between the catalytic domain and the carboxyl tail, to obtain maximal enzymatic activity (26). Interestingly, phosphorylation at several Ser/Thr residues within the C-terminal autoinhibitory tail appears to either activate or inhibit S6K1, depending on the cell cycle phase. Shah *et al.* (27) demonstrated that phosphorylation of those residues (featured by the Thr-421/Ser-424 site) during mitosis pursued by Cdk1 inactivates S6K1 to terminate protein synthesis prior to cell division (28). A recent report by Schmidt *et al.* (29) demonstrating that phosphorylation of Thr-421/Ser-424 is specifically increased during the G_2/M phase may also support the finding, whereas during the G_1 phase, there is consensus that the phosphorylation at the autoinhibitory domain is requisite for S6K1 activation (26), as also recently demonstrated by Hou *et al.* (30), where the Cdk5 phosphorylates the Ser-411 site, leading to activation of S6K1. In contrast to such inhibitory regulation of S6K1 during mitosis, however, a recent report by Boyer *et al.* (31) sharply demonstrated that the activity of S6K1 peaks at mitosis, suggesting that S6K1 may also have some roles during the mitotic phase. If so, how its activity is supported against the inhibitory regulation caused by Cdk1 remains an open question.

Hence, the two observations above that both DEDD$^{-/-}$ and S6K1$^{-/-}$ situations decrease the efficacy of ribosome and protein synthesis, resulting in smaller cell and body size, and that mitotic Cdk1 has a functional interaction with both S6K1 and DEDD led us here to assess a possible role of DEDD in the context of the functional regulation of S6K1.

EXPERIMENTAL PROCEDURES

Mice—DEDD$^{-/-}$ mice (10) had been backcrossed to C57BL/6 (B6) for 17 generations before they were used in experiments. Mice were maintained under a specific pathogen-free condition.

Antibodies—Antibodies used for experiments are as follows: anti-S6K1 phosphorylated at Thr-421/Ser-424, anti-S6K1 phosphorylated at Thr-389, anti-total rpS6 (clone 54D2), anti-rpS6 phosphorylated at Ser-240/244, anti-total Akt (clone 11E7), anti-Akt phosphorylated at Thr-308 (clone 244F9) (all are from Cell Signaling Technology, Beverly, MA); anti-S6K1 phosphorylated at Ser-411 (clone SC-7983R), anti-α-tubulin and anti-insulin (clone H-86) (from Santa Cruz Biotechnology, Inc., Santa Cruz, CA); anti-cyclin B1 (clone GNS-11) and anti-total S6K1 (clone 16) (from BD Biosciences); anti-Hsp90 (clone SPA-830) and anti-Cdk1 (clone A17) (from Stressgen (Victoria, Canada) and Zymed Laboratories Inc. (South San Francisco, CA)).

S6K1 Kinase Assay—DEDD$^{+/+}$ or DEDD$^{-/-}$ mouse embryonic fibroblast (MEF) cells were lysed in lysis buffer (20 mM Tris-HCl, pH 7.5, 50 mM NaCl, 1 mM Na_3VO_4, 50 mM NaF, 5 mM EDTA, 0.1% Nonidet P-40, supplemented with a mixture of protease inhibitors). The cell lysates were clarified by centrifugation for 30 min at 14,000 rpm and immunoprecipitated with anti-S6K1 antibody preabsorbed to protein G-agarose beads at 4 °C for 4 h. The immune complexes were washed twice with lysis buffer and once with kinase assay buffer (20 mM Tris-HCl, pH 7.5, 10 mM $MgCl_2$, 0.1 mg/ml bovine serum albumin, and 0.4 mM dithiothreitol). The kinase reaction was performed at 30 °C for 15 min in the presence of 100 μM ATP, 200 μCi/ml [γ-^{32}P]ATP, and 125 μM S6 peptide substrate (RRRLSSLRA; Upstate Biotechnology Inc., Lake Placid, NY) and was terminated by the addition of 20 μl of 250 mM EDTA and boiling for 5 min. Stopped reactions were loaded onto P-81 phosphocellulose membrane (Whatman, Maidstone, UK) and were washed with 75 mM phosphoric acid. The labeled probe was measured by liquid scintillation counting.

siRNA Transfection—Double-stranded siRNA targeting DEDD or Cdk1 were purchased from Applied Biosystems or Sigma, respectively. Wild-type MEF cells at a 50% confluent state were transfected with 10 μM siRNA using Lipofectamine 2000 (Invitrogen). Forty-eight hours after transfection, the cells were harvested and analyzed by Western blotting or reverse transcription-PCR. Sequences of the oligonucleotides were as follows: DEDD siRNA 1, 5-GCCCTGATCTTGTAGACAATT-3; DEDD siRNA 2, 5-AAATGGACGTGACTTCTTATT-3; Cdk1 siRNA 1, 5-CTATGATCCTGCCAAACGATT-3; Cdk1 siRNA 2, 5-GTTGTTACCGTTGGCTCTTT-3; Cdk1 siRNA 3, 5-CAATCAAACTGGCTGATTTTT-3. As a control, an oligonucleotide targeting the GFP sequence (Sigma) was used.

In Vitro Binding Assay—Glutathione *S*-transferase (GST)-fusion proteins containing mouse DEDD, Cdk1, cyclin B1, or S6K1 were produced in *Escherichia coli* M15 carrying pGEX-5X1-DEDD, Cdk1, cyclin B1, or S6K1. These proteins were purified according to protocols described in the GST·Bind kit instructions (Novagen, Madison, WI). V5-DEDD, Myc-cyclin B1, or HA-Cdk1 was efficiently expressed in the baculovirus/High Five cell system (Invitrogen). In each binding assay, 200 ng of GST fusion proteins or 100 μl of High Five cell lysates were used. GST fusion proteins or High Five cell extracts were incubated with the anti-S6K1 or anti-cyclin B1 antibodies in lysis buffer (20 mM Tris-HCl, pH 7.5, 50 mM NaCl, 5 mM $MgCl_2$, 1 mM Na_3VO_4, 25 mM NaF, 1 mM phenylmethylsulfonyl fluoride, 0.1% Nonidet P-40, supplemented with a mixture of protease inhibitors) at 4 °C for 4 h and precipitated with protein G-Sepharose beads (Sigma). The pellets were washed three times with lysis buffer. The immunoprecipitates and total cell lysates were analyzed by Western blotting using anti-DEDD antibody. Note that the anti-DEDD antibody was newly generated by us and that this antibody is available for recognition of recombinant DEDD, but not of endogenous DEDD by immunoblotting.

Islet Isolation and Insulin Content—Isolation of islets from mice and assessment of insulin content within islet cells were carried out as described previously (32). Briefly, after clamping the common bile duct at a point close to its opening into the duodenum, liberase RI (Roche Applied Science) was injected into the pancreatic duct. The swollen pancreas was removed and incubated at 37 °C for 24 min. The pancreas was dispersed

by pipetting, and dispersed cells were washed twice. Islets were manually collected through a stereoscopic microscope. These islets were used for the experiments immediately after isolation. Insulin content was measured as described previously (32). Isolated islets were extracted in acid ethanol at −20 °C, and after preincubation with the basal glucose concentration for 20 min, static incubation of 10 islets/tube was performed at 37 °C for 1 h. Insulin levels were determined with an insulin enzyme-linked immunosorbent assay kit (Morinaga).

Primers for Reverse Transcription-PCR—Primers used are as follows: Hsp90α, 5-GCGGCAAAGACAAGAAAAAG-3 (forward) and 5-CAAGTGGTCCTCCCAGTCAT-3 (reverse); Hsp90β, 5-CTGGGTCAAGCAGAAAGGAG-3 (forward) and 5-TCTCTGTTGCTTCCCGACTT-3 (reverse); Akt1, 5-CCACGCTACTTCCTCCTC-3 (forward) and 5-TGCCCTTGCCAACAGTCTGAAGCA-3 (reverse); Akt2, 5-GTCGCCAACAGTCTGAAGCA-3 (forward) and 5-GAGAGAGGTGGAAAAACAGC-3 (reverse); G3PDH, 5-ACCACAGTCCATGCCATCAC-3 (forward) and 5-TCCACCACCCTGTTGCTGTA-3 (reverse); β-actin, 5-GTGGCTACAGCTTCACCACCACAG-3 (forward) and 5-GCATCCTGTCAGCAATGCCTGGGT-3 (reverse); DEDD, 5-GCGGGATCCGCGGGCCTAAAGAGGC-3 (forward) and 5-GCGTCTAGAGTCTACAAGATCAGGGC-3 (reverse).

Quantification of Immunoblots—Quantification of the immunoblots was performed using NIH Image. Relative phosphorylation levels to those in control (shown as 1.0 ± S.E.) are presented. For all immunoblotting experiments, at least three independent blots were performed.

Statistical Analysis—A two-tailed Mann-Whitney test was used to calculate p values. **, $p < 0.01$; *, $p < 0.05$; *error bars*, S.E.

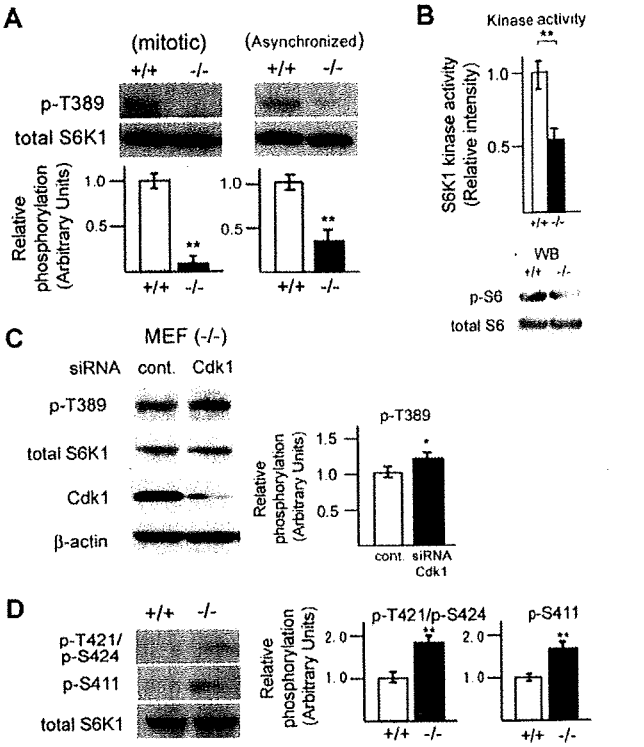

FIGURE 1. **Absence of DEDD decreases S6K1 activity.** *A*, phosphorylation (*p-*) at Thr-389 of S6K1 in DEDD$^{+/+}$ or DEDD$^{-/-}$ MEF cells, tested by Western blotting. *B* (*top*), kinase activity of S6K1 precipitated from DEDD$^{+/+}$ or DEDD$^{-/-}$ MEF cells. Results were normalized by the average of those for DEDD$^{+/+}$ cells. *Error bar*, S.E. *Bottom*, phosphorylation at rpS6 in DEDD$^{+/+}$ or DEDD$^{-/-}$ MEF cells, tested by Western blotting (*WB*). *C*, knockdown of Cdk1 increased phosphorylation at Thr-389 of S6K1 in mitotic DEDD$^{-/-}$ MEF cells. *D*, phosphorylation at Thr-421/Ser-424 and Ser-411 of S6K1 in mitotic DEDD$^{+/+}$ or DEDD$^{-/-}$ MEF cells.

RESULTS AND DISCUSSION

DEDD Prevents Inhibitory Phosphorylation of Mitotic S6K1 and Supports Its Activity—To test if DEDD is involved in regulation of S6K1 activity, we first investigated whether the lack of DEDD influences S6K1 activity. Significantly, levels of phosphorylation at Thr-389 of S6K1, a hallmark of active S6K1, was attenuated in DEDD$^{-/-}$ compared with DEDD$^{+/+}$ MEF cells that had been enriched in the mitotic phase by a nocodazole block (Fig. 1*A*, *left*). Interestingly, reduction in Thr-389 phosphorylation was also observed in asynchronized DEDD$^{-/-}$ MEF cells (Fig. 1*A*, *right*). Thus, such a DEDD activating effect on S6K1 at the mitotic phase appears to influence the overall S6K1 activity in cells. Furthermore, a kinase activity assay based on the incorporation of ^{32}P-labeled ATP demonstrated that S6K1 precipitated from DEDD$^{-/-}$ MEF cells had 50% less activity on a specific substrate of S6K1, rpS6, compared with that from DEDD$^{+/+}$ cells (442.54 ± 30.79 (−/−) *versus* 850.67 ± 26.63 (+/+) cpm normalized by the amount of precipitated S6K1 protein; Fig. 1*B* (*top*) shows a summary of data). This result was also supported by a reduction in phosphorylation levels of rpS6 in DEDD$^{-/-}$ compared with DEDD$^{+/+}$ MEF cells, when assessed by Western blotting (Fig. 1*B*, *lower panels*). The reduction of the rpS6 phosphorylation level in the absence of DEDD was less remarkable than expected by the result from the kinase activity assay. This might be due to a possible functional redundancy caused by S6K2 in the phosphorylation of rpS6 (33).

Since DEDD suppresses mitotic Cdk1 (10), increased Cdk1 activity in the absence of DEDD might enhance the inhibitory regulation of S6K1, leading to less S6K1 activity in DEDD$^{-/-}$ cells. Supporting this hypothesis, suppression of Cdk1 via siRNA expression increased Thr-389 phosphorylation in DEDD$^{-/-}$ cells (Fig. 1*C*). We then assessed the phosphorylation status of the mitosis-specific inhibitory residue of S6K1, Thr-421/Ser-424, which is targeted by mitotic Cdk1. As presented in Fig. 1*D*, phosphorylation at Thr-421/Ser-424 was enhanced in mitotic DEDD$^{-/-}$ MEF cells compared with DEDD$^{+/+}$ MEF cells. In brief, in the absence of DEDD, the activity of S6K1 was substantially diminished due to hyperphosphorylation at the inhibitory Ser/Thr residues. The phosphorylation level at Ser-411 (also within the autoinhibitory tail) was also increased in DEDD$^{-/-}$ cells (Fig. 1*D*). Although this result is consistent with the observation by Shah *et al.* (28) suggesting the presence of multiple Cdk1-dependent inhibitory phosphorylation sites, whether the mitotic phosphorylation at Ser-411 certainly decreases S6K1 activity remains arguable.

DEDD Associates with S6K1 through Its Proline-rich Region—We then tested whether DEDD associates with S6K1. We expressed FLAG-tagged DEDD in 293T cells and assessed whether S6K1 is co-precipitated with DEDD. Remarkably,

S6K1 was bound to DEDD (Fig. 2*A*). Moreover, S6K1 co-precipitated with DEDD was deficient in phosphorylation at both Thr-421/Ser-424 and Ser-411, whereas the Thr-389 site was phosphorylated, suggesting that the association of DEDD with S6K1 prevents inhibitory phosphorylation of S6K1 that is caused by mitotic Cdk1 (Fig. 2*A*). An *in vitro* assay using tagged recombinant proteins supported the notion that DEDD associates with S6K1 through Cdk1-cyclin B1, since DEDD was co-precipitated with S6K1 only in the presence of both Cdk1 and cyclin B1 (Fig. 2*B*).

Next, in order to determine the region involved in the association of DEDD with S6K1, we designed a number of variant DEDD molecules (Fig. 2*C*) and tested their association with S6K1. As depicted in Fig. 2*D*, a DEDD variant lacking the proline-rich region did not bind to S6K1, indicating a requirement of the proline-rich region of DEDD for the association with S6K1. Note that in multiple experiments, the expression level of the V2 DEDD variant was lower compared with that of other types when expressed in 293 cells (Fig. 2*D*, *bottom*). It is possible that the V2 DEDD variant may be structurally unstable.

Reduction in β Cell Size and Insulin Mass Due to Decreased S6K1 Activity in DEDD$^{-/-}$ Pancreas—S6K1 is involved in control of glucose tolerance by supporting the size of insulin-producing β cells in the pancreas (21). As shown in Fig. 3*A*, the association of DEDD with S6K1 was certainly observed in β cells when tested using a mouse pancreatic β cell line, MIN6 (34). In line with this finding, activating phosphorylation of S6K1 at Thr-389 was significantly decreased in these cells when DEDD was knocked down by siRNA expression (Fig. 3*B*).

Also *in vivo*, diminishment of S6K1 phosphorylation at the Thr-389 site was apparent in the DEDD$^{-/-}$ pancreas compared with the DEDD$^{+/+}$ pancreas (Fig. 3*C*). Furthermore, the DEDD$^{-/-}$ pancreas also exhibited an increase in phosphorylation levels at Thr-421/Ser-424 and Ser-411 residues, as seen in MEF cells (Fig. 3*D*). We then assessed whether pancreatic islets

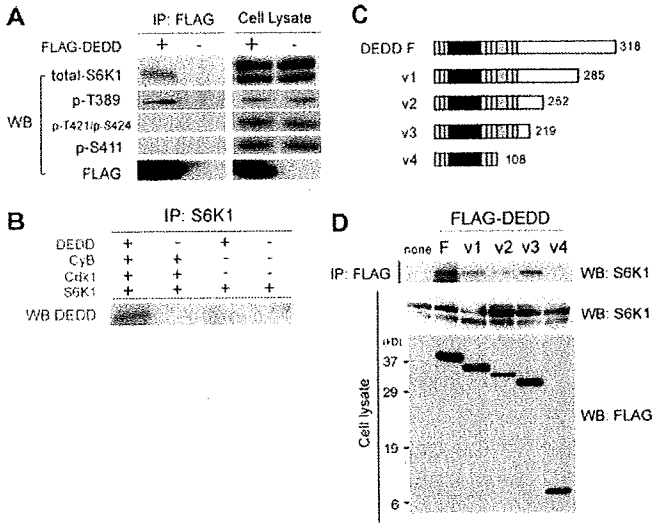

FIGURE 2. **DEDD forms a complex with S6K1 and Cdk1 via its proline-rich region.** *A*, co-immunoprecipitation (*IP*) of FLAG-tagged DEDD (*FLAG-DEDD*) and S6K1, using anti-FLAG antibody. Precipitates were analyzed for the indicated items. Western blots (*WB*) of cell lysates for respective subjects are also presented. Note in 293T cell lysates, protein blot for total S6K1 using a mouse monoclonal antibody (clone 16; BD Biosciences) reveals double bands, as previously described (40, 41). *B*, *in vitro* binding assay using recombinant proteins. *C*, schematic diagram of the structure of DEDD variants. *Light blue region*, nuclear localizing signal; *black region*, DED domain; *orange region*, proline-rich region. The *numbers* indicate amino acids starting from the first methionine. *D*, co-immunoprecipitation of S6K1 and FLAG-tagged DEDD variants, using an anti-FLAG antibody.

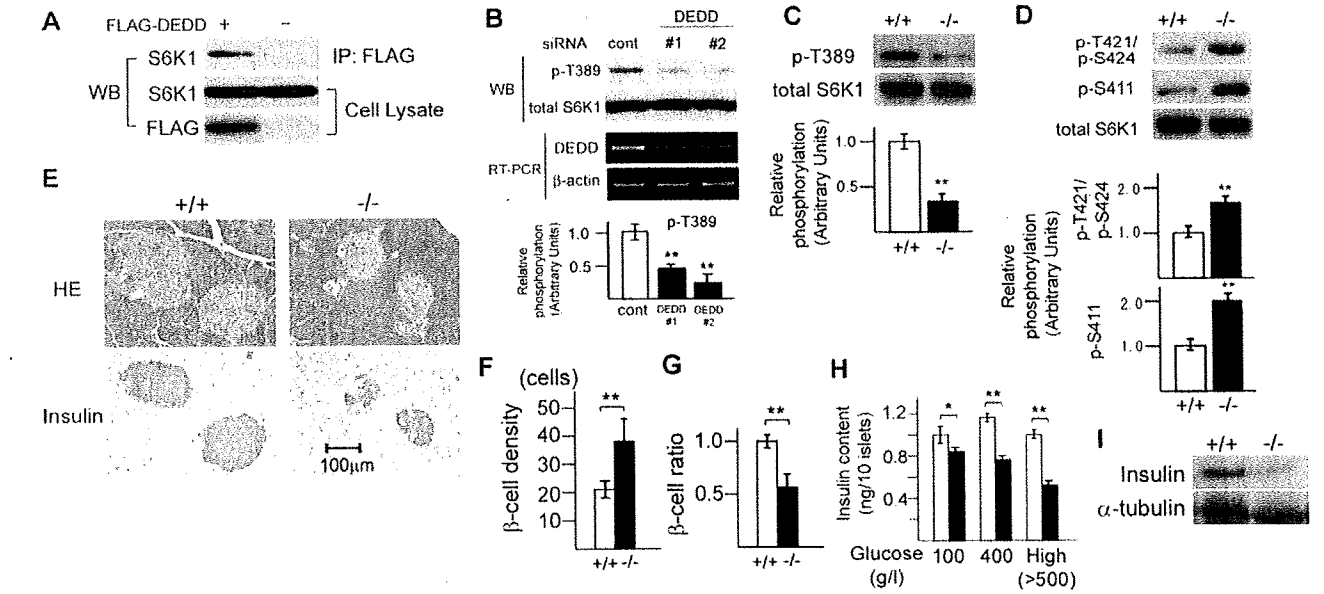

FIGURE 3. **Decreased insulin mass within pancreatic islets in DEDD$^{-/-}$ mice.** *A*, co-immunoprecipitation (*IP*) of FLAG-DEDD and S6K1 in MIN6 cell lysates. *B*, DEDD knockdown decreased phosphorylation levels at the Thr-389 residue of S6K1 in MIN6 cells. Down-regulation of DEDD mRNA expression is also shown (reverse transcription-PCR; *RT-PCR*). *C* and *D*, phosphorylation at Thr-389 residue (*C*) or Thr-421/Ser-424 and Ser-411 (*D*) of S6K1 in DEDD$^{+/+}$ or DEDD$^{-/-}$ pancreas. *E*, histological analysis of pancreatic Langerhans islets. *Top*, HE staining; *bottom*, immunostaining for insulin. *F*, β cell density assessed by the number of nuclei per 2.5 × 10^3 μm^2 within the insulin-positive area. Ten independent islets for each genotype were analyzed. *G*, the ratio of insulin-stained area per whole islet. Twenty islets for each type of mice were analyzed. Results were normalized by the average of those for DEDD$^{+/+}$ mice. *H*, insulin content. Islets were isolated from DEDD$^{+/+}$ or DEDD$^{-/-}$ pancreas (four for each), and the insulin content within islets was analyzed. Data are averages of five groups of 10 islets. *Error bar*, S.E. The concentration of glucose used for incubation was 100 or 400 g/liter or higher (*High*). *I*, Western blotting (*WB*) for insulin using pancreas protein.

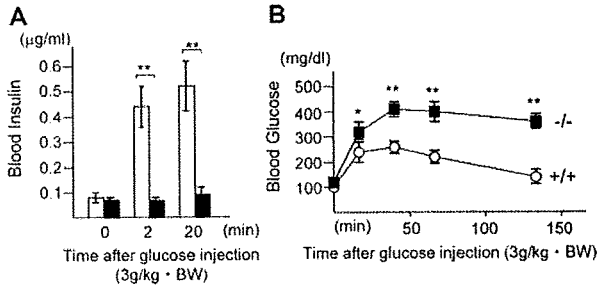

FIGURE 4. **Glucose intolerance in DEDD$^{-/-}$ mice.** *A*, serum insulin levels after a glucose challenge. $n = 5$ each. *Black bars*, DEDD$^{-/-}$ mice; *white bars*, DEDD$^{+/+}$ mice. *B*, blood glucose levels after glucose administration (3 g/kg body weight (*BW*)). Male DEDD$^{-/-}$ and their littermate DEDD$^{+/+}$ mice at 6–8 weeks of age were used. $n = 8$ each. *Black boxes*, DEDD$^{-/-}$ mice; *white circles*, DEDD$^{+/+}$ mice.

were smaller in DEDD$^{-/-}$ mice than in DEDD$^{+/+}$ mice, as seen in S6K1$^{-/-}$ mice. According to histological analysis, the size of each β cell was reduced in DEDD$^{-/-}$ mice (Fig. 3*E*, *top two panels*), as also indicated by a higher density of β cells within the islet (Fig. 3*F*). Similarly, the insulin mass, determined by the ratio of β cells to whole islet mass after immunostaining of pancreatic sections for insulin, was reduced by 50% in DEDD$^{-/-}$ mice (Fig. 3, *E* (*bottom two panels*) and *G*). In agreement with this observation, insulin content within β cells from DEDD$^{-/-}$ mice was significantly decreased when assessed by *in vitro* measurement using isolated pancreatic islets (Fig. 3*H*). Furthermore, Western blot analysis demonstrated that the amount of insulin in the pancreas of DEDD$^{-/-}$ mice was decreased compared with that in the DEDD$^{+/+}$ pancreas (Fig. 3*I*). Finally, Tdd-mediated dUTP-biotin nick-end labeling staining of the pancreas sections did not reveal any difference in DEDD$^{-/-}$ and DEDD$^{+/+}$ islets, suggesting no influence of the lack of DEDD on apoptosis of islet cells (data not shown).

Attenuated Insulin Secretion upon Glucose Stimulation in DEDD$^{-/-}$ Mice—Last, we assessed insulin secretion and glucose tolerance in DEDD$^{-/-}$ mice *in vivo*. To this end, we first kinetically analyzed the blood insulin levels in response to glucose administration after mice were fasted for 2 h. As expected from the overt reduction in β cell size and insulin content (presented in Fig. 3), insulin levels were less elevated at 2 or 20 min after the glucose challenge in DEDD$^{-/-}$ mice compared with DEDD$^{+/+}$ mice (Fig. 4*A*). Such inefficient insulin secretion in DEDD$^{-/-}$ mice resulted in glucose intolerance. As shown in Fig. 4*B*, at early times after the glucose challenge, blood glucose levels were more than 150% higher in DEDD$^{-/-}$ than in DEDD$^{+/+}$ mice, although they were comparable in both types of mice before glucose administration (Fig. 4*B*). Two hours after the injection of glucose, when the blood glucose level decreased to the initial level in DEDD$^{+/+}$ mice, it was still twice as high as that under the fasted condition in DEDD$^{-/-}$ mice (Fig. 4*B*). Thus, like in S6K1$^{-/-}$ mice, DEDD$^{-/-}$ mice suffered glucose intolerance due to inefficient insulin secretion upon glucose stimulation, which is accounted for by a reduction in insulin mass in pancreatic islets.

Conclusion—In this report, we demonstrated that DEDD is required for preservation of S6K1 activity during mitosis and that this reaction increases overall S6K1 activity in cells. This finding may suggest that the maintenance of mitotic S6K1 activity by the time of cytokinesis appears to be important to gain efficient cell and body size in mammals. This scenario is consistent with the observation by Boyer *et al.* (31), in which S6K1 activity achieves the maximal levels in the mitotic phase. As in our previous finding (10), DEDD appears to be involved in cell growth control prior to cell division via different mechanisms (*i.e.* impediment of mitosis progression and maintenance of S6K1 activity). Importantly, both effects are achieved through suppression of mitotic Cdk1, although further studies are required to fully understand the mechanism of how DEDD suppresses mitotic Cdk1 activity. Nonetheless, such new insights may further implicate the mitotic phase during the cell cycle as a crucial period involved in balancing mammalian cell size.

Although the DED-containing molecules were initially supposed to be involved in apoptosis regulation, evidence has accumulated that they have diverse functions (35, 36). For instance, Arechiga *et al.* (37) reported that FADD and caspase-8, also DED-containing family members, play essential roles in maintaining S6K1 activity during G_1/S phases by modulating Cdk2 in T cells. Likewise, RIP1 (receptor-interacting protein 1), also a DED-containing kinase that mediates NFκB activation, regulates $p27^{Kip1}$ levels through the PI3K-Akt-forkhead pathway, thereby promoting the G_1/S transition (38). Together with our findings of the effects of DEDD in the mitotic phase, these observations may corroborate that the DED-containing elements appear to be widely involved in the control of the PI3K-signaling cascade as well as in the progression of different cell cycle phases. Because the PI3K pathway is crucial in the regulation of cell metabolisms, further studies might investigate the role of DED-containing proteins in various metabolic diseases. Since DEDD$^{-/-}$ mice revealed glucose intolerance, it might be worthwhile to assess whether any dysfunction of DEDD is present, either in the whole body or in specific tissues, in a subset of type 2 diabetes patients. Schumann *et al.* (39) reported that the Fas pathway, where many DED-containing elements are associated, is involved in β cell secretory function. Thus, DED-containing proteins might also influence metabolic homeostasis through apoptosis cascades, although DEDD$^{-/-}$ cells or mice showed no apparent defect in apoptosis (10, 11). Future analyses will clarify this issue more precisely.

Acknowledgments—We thank Drs. I. Takamoto, T. Kubota, M. Tsunoda, M. Kaneko, and Genostaff Inc. (in particular, K. Ohkubo) and Tosoh Corp. for technical assistance; Dr. J.-I. Miyazaki for MIN6 cells; and M. Egami for preparing the manuscript.

REFERENCES

1. Conlon, I., and Raff, M. (1999) *Cell* **96**, 235–244
2. Montagne, J. (2000) *Mol. Cell. Biol. Res. Commun.* **4**, 195–202
3. Cooper, S. (2004) *BMC Cell Biol.* **5**, 35
4. Jorgensen, P., and Tyers, M. (2004) *Curr. Biol.* **14**, 1014–1027
5. De Virgilio, C., and Loewith, R. (2006) *Oncogene* **25**, 6392–6415
6. Jorgensen, P., Nishikawa, J. L., Breitkreutz, B. J., and Tyers, M. (2002) *Science* **297**, 395–400
7. Rupes, I. (2002) *Trends Genet.* **18**, 479–485
8. Kellogg, D. R. (2003) *J. Cell Sci.* **116**, 4883–4890
9. Jorgensen, P., Rupes, I., Sharom, J. R., Schneper, L., Broach, J. R., and Tyers, M. (2004) *Genes Dev.* **18**, 2491–2505